Characterization of Kcnk3 -Mutated Rat, a Novel Model of Pulmonary Hypertension

Mélanie Lambert, Véronique Capuano, Angele Boet, Laurent Tesson, Thomas Bertero, Morad Nakhleh, Séverine Remy, Ignacio Anegon, Christine Péchoux, Aurélie Hautefort, et al.

Circulation Research

ORIGINAL RESEARCH

Characterization of *Kcnk3*-Mutated Rat, a Novel Model of Pulmonary Hypertension

Mélanie Lambert, Véronique Capuano, Angèle Boet, Laurent Tesson, Thomas Bertero, Morad K. Nakhleh, Séverine Remy, Ignacio Anegon, Christine Pechoux, Aurélie Hautefort, Catherine Rucker-Martin, Boris Manoury, Valérie Domergue, Olaf Mercier, Barbara Girerd, David Montani, Frédéric Perros, Marc Humbert, Fabrice Antigny

RATIONALE: Pulmonary arterial hypertension is a severe lethal cardiopulmonary disease. Loss of function mutations in *KCNK3* (potassium channel subfamily K member 3) gene, which encodes an outward rectifier K^+ channel, have been identified in pulmonary arterial hypertension patients.

OBJECTIVE: We have demonstrated that KCNK3 dysfunction is common to heritable and nonheritable pulmonary arterial hypertension and to experimental pulmonary hypertension (PH). Finally, KCNK3 is not functional in mouse pulmonary vasculature.

METHODS AND RESULTS: Using CRISPR/Cas9 technology, we generated a 94 bp out of frame deletion in exon 1 of *Kcnk3* gene and characterized these rats at the electrophysiological, echocardiographic, hemodynamic, morphological, cellular, and molecular levels to decipher the cellular mechanisms associated with loss of KCNK3. Using patch-clamp technique, we validated our transgenic strategy by demonstrating the absence of KCNK3 current in freshly isolated pulmonary arterial smooth muscle cells from *Kcnk3*-mutated rats. At 4 months of age, echocardiographic parameters revealed shortening of the pulmonary artery acceleration time associated with elevation of the right ventricular systolic pressure. *Kcnk3*-mutated rats developed more severe PH than wild-type rats after monocrotaline exposure or chronic hypoxia exposure. *Kcnk3*-mutation induced a lung distal neomuscularization and perivascular extracellular matrix activation. Lungs of *Kcnk3*-mutated rats were characterized by overactivation of ERK1/2 (extracellular signal–regulated kinase1-/2), AKT (protein kinase B), SRC, and overexpression of HIF1-α (hypoxia-inducible factor-1 α), survivin, and VWF (Von Willebrand factor). Linked with plasma membrane depolarization, reduced endothelial-NOS expression and desensitization of endothelial-derived hyperpolarizing factor, *Kcnk3*-mutated rats presented predisposition to vasoconstriction of pulmonary arteries and a severe loss of sildenafil-induced pulmonary arteries relaxation. Moreover, we showed strong alteration of right ventricular cardiomyocyte excitability. Finally, *Kcnk3*-mutated rats developed age-dependent PH associated with low serum-albumin concentration.

CONCLUSIONS: We established the first *Kcnk3*-mutated rat model of PH. Our results confirm that KCNK3 loss of function is a key event in pulmonary arterial hypertension pathogenesis. This model presents new opportunities for understanding the initiating mechanisms of PH and testing biologically relevant therapeutic molecules in the context of PH.

VISUAL OVERVIEW: An online visual overview is available for this article.

Key Words: echocardiography ■ exon ■ extracellular matrix ■ hypoxia ■ rats

Editorial, see p 696 | In This Issue, see p 659 | Meet the First Author, see p 660

Pulmonary arterial hypertension (PAH) is an uncommon, progressive, and severe disease with an estimated prevalence of 15 to 50 per million.[1] PAH has been hemodynamically defined by an elevation of the mean pulmonary artery pressure >20 mm Hg and pulmonary vascular resistance >3 Wood units at rest.[2] PAH results from increased pulmonary vascular resistance because of remodeling of the small distal pulmonary arteries (PAs) and arterioles (diameter <500 µm), causing adaptive right ventricular (RV) hypertrophy and

Correspondence to: Fabrice Antigny, INSERM UMR_S 999, Hôpital Marie Lannelongue, 133, Ave de la Résistance, F-92350 Le Plessis Robinson, France. Email fabrice.antigny@u-psud.fr

The online-only Data Supplement is available with this article at https://www.ahajournals.org/doi/suppl/10.1161/CIRCRESAHA.119.314793.

For Sources of Funding and Disclosures, see page 694.

Circulation Research is available at www.ahajournals.org/journal/res

Novelty and Significance

What Is Known?

- Loss of function mutations in the *KCNK3* (potassium channel subfamily K member 3) gene have been described in pulmonary arterial hypertension (PAH) patients and those who are carriers of *KCNK3* mutations are younger as compared with idiopathic PAH patients.
- Reduced KCNK3 expression/function is common to heritable and nonheritable PAH and to experimental pulmonary hypertension.
- KCNK3 is not functional in mouse pulmonary arterial smooth muscle cell limiting previous mechanistic exploration.

What New Information Does This Article Contribute?

- By CRISPR/Cas9 technology, we generate *Kcnk3*-mutated rats to inactivate the KCNK3 channel.
- At 4 months old, *Kcnk3*-mutated rats develop spontaneous elevation of right ventricular systolic pressure, are sensitized to induced pulmonary hypertension (monocrotaline or chronic hypoxia), and develop age-dependent pulmonary hypertension at 12 months.
- *Kcnk3* dysfunction leads to distal pulmonary vessels neomuscularization and perivascular collagen deposition associated with overactivation of proproliferative pathways (ERK1/2 [extracellular signal–regulated kinase1-/2] and HIF-1α [hypoxia-inducible factor-1 α]) and endothelial phenotype switch.
- We identify that an increase of HIF1-α and ERK1/2 are the primary molecular events linked to *Kcnk3*-dysfunction.
- Pulmonary arteries from *Kcnk3*-mutated rats are sensitized to constriction and are less responsive to vasorelaxing stimuli.

Pulmonary arterial hypertension (PAH) is a progressive and severe disease. Since 2013, several loss of function mutations in *KCNK3* gene have been detected in select PAH patients. *KCNK3* encodes an outward-K^+ channel member of the 2-pore K^+ channel family. Patients with the *KCNK3* mutation are younger at diagnosis than idiopathic PAH patients. Loss of function and expression is a hallmark of PAH at pulmonary vascular and right ventricular levels. However, the mechanisms linking *KCNK3* dysfunction with PAH were unknown. Using unique *Kcnk3*-mutated rats and human pulmonary arterial smooth muscle cells we aimed to decipher the cellular mechanisms associated with KCNK3-dysfunction. Our results demonstrate that KCNK3 loss of function is a key event in PAH pathogenesis. Using a combination of hemodynamic measurements, molecular biology, histological analyses, and electrophysiology approaches, we show that KCNK3-dysfunction leads to plasma membrane depolarization, pulmonary arterial smooth muscle cells overproliferation, ERK1/2 and HIF1-α over-activation, mitochondrial depolarization, pulmonary artery vasoconstriction, pulmonary vessels remodeling, endothelial cell phenotype switch, and reduction of RV cardiomyocytes excitability. These results highlight that KCNK3 loss of function is consistent with human PAH pathobiology and demonstrate that KCNK3-dysfunction is a key events in PAH. This model presents new opportunities for understanding the initiating mechanisms of pulmonary hypertension.

Nonstandard Abbreviations and Acronyms

α-SMA	α-smooth muscle actin
CH	chronic hypoxia
ECM	extracellular matrix
EDHF	endothelium-derived hyperpolarizing factor
HIF1-α	hypoxia-inducible factor-1 α
MCT	monocrotaline
NOS	nitric oxide synthase
PA	pulmonary artery
PAH	pulmonary arterial hypertension
PASMC	pulmonary arterial smooth muscle cell
PH	pulmonary hypertension
RVSP	right ventricular systolic pressure
TPR	total pulmonary resistance
VWF	Von Willebrand factor
WT	wild type

when unchecked, right heart failure.[3] In 2013, whole-exome sequencing revealed 6 types of heterozygous mutations in *KCNK3* (potassium channel subfamily K member 3), representing the first channelopathy identified in PAH.[4] In 2016, Navas et al[5] identified 2 additional *KCNK3* mutations in PAH patients and described the first PAH patient with a homozygous *KCNK3* mutation associated with an aggressive form of PAH and early disease development.[4] Finally, in 2017, 2 new mutations were identified in an Asian and an American cohort of PAH patients.[6,7] *KCNK3* mutations carriers' patients are younger at diagnosis than idiopathic PAH patients and have a higher mean pulmonary artery pressure.[8]

KCNK3 encodes an outward-K^+ channel member of the 2 pore K^+ channel family, characterized by 4 transmembrane domains and 2 pore domains per subunit.[4] KCNK3 channel, also known as TASK-1 (Twik-related-acid-sensitive-K^+ channel) or K2P3.1[9] participates in regulating resting membrane potential in several cell types including human pulmonary arterial smooth muscle cells

(PASMCs).[8] Electrophysiological recording demonstrated a loss of function for all *KCNK3* mutations identified.[4] We recently determined that KCNK3 dysfunction contributes to the development of heritable PAH (*BMPR2* mutated patients) and idiopathic PAH, indicating that KCNK3 dysfunction is a hallmark of PAH at pulmonary vascular and RV levels.[10,11] However, the mechanisms linking *KCNK3* dysfunction with PAH are still unknown. Contrary to rats where KCNK3 is functionally expressed in pulmonary vasculature,[10] mice are not a suitable models to study the role of KCNK3 in pulmonary hypertension (PH) as KCNK3 does not form a functional channel in mouse PASMCs[12] and is replaced by KCNK6 channel.[13] Therefore, we developed the first *Kcnk3*-mutated rat line to decipher the role of KCNK3 dysfunction in the context of PAH pathobiology, representing an interesting model to study the time-dependent cellular and molecular mechanisms involved in PH development.

Using a combination of hemodynamic measurements, molecular biology, histological analyses, and electrophysiology approaches, we characterized the first *Kcnk3*-mutated rat model, providing tools for developing specific therapeutic targets for PH.

METHODS

The authors declare that all supporting data are available within the article and its Online Data Supplement.

Because of space limitations, a detailed description of the Materials and Methods is presented in the Online Data Supplement.

RESULTS

KCNK3 Current Is Absent in Freshly isolated PASMCs From Kcnk3-Mutated Rats

Kcnk3-mutated Sprague-Dawley rats were generated using CRISPR-Cas9 system with a specific sgRNA-rKCNK3 and Cas9 mRNA,[14] targeting the first exon of *Kcnk3* gene. In one of the newborn rats, a deletion of 94 bp (Δ94ex1) was found, which originated an out of frame shift in the open reading frame that leads to a premature stop codon and the generation of a completely different aa (amino acid) sequence (Figure 1A). Although premature stop codon may generate a degradation of the mRNA,[15] we showed the presence of a mutated mRNA deleted of 94 bp but not its absence (Figure 1B) suggesting an absence of nonsense mRNA degradation pathway as already mentioned elsewhere.[15] Nevertheless, a putative translation of the truncated mRNA could produce a truncated 90-aa protein instead of the 411 aa of the wild-type (WT) protein (Figure 1A) and share only the first 14 aa in common with the WT protein. The sequencing of the *Kcnk3* mRNA from $Kcnk3^{+/+}$ and $Kcnk3^{\Delta 94ex1/\Delta 94ex1}$ rats confirmed the deletion of the 94 bp and an aberrant potential protein sequence with 8 potential premature stop codons (Online Figure I).

The founder animal with the Δ94ex1 mutation was crossed with a WT partner, and the mutation was transmitted to the offspring as shown by genotype DNA analysis, demonstrating that the rats were either $Kcnk3^{+/+}$, heterozygous $Kcnk3^{\Delta 94ex1/+}$, or homozygous $Kcnk3^{\Delta 94ex1/\Delta 94ex1}$ (Figure 1C). Unfortunately, there is no available specific antibodies for KCNK3,[16,17] thus avoiding any measurement of the protein expression of KCNK3 in *Kcnk3*-mutated rats. We showed that all commercially anti-KCNK3 antibodies tested were unusable because when tested in *Kcnk3*-knockout mice, they were either nonreactive or gave the same signal as in the WT mice (Online Figure II and IIbis). The same unspecific staining occurred in *Kcnk3*-mutated rats. Thus, we could not assert the absence of KCNK3 protein in *Kcnk3*-mutated rats. Nevertheless, whole cell patch-clamp measurement on freshly isolated PASMCs from WT and *Kcnk3*-mutated rats clearly showed a defect in KCNK3 current in mutated rats. Indeed, the global-K^+ current was significantly reduced: 50% in $Kcnk3^{\Delta 94ex1/+}$ rats and 60% in $Kcnk3^{\Delta 94ex1/\Delta 94ex1}$rats compared with the WT (Figure 1D and 1E). We then specifically measured the KCNK3 current (I_{KCNK3}) after applying a specific KCNK3 channel inhibitor (A293 at 200 nmol/L)[10] and defined it as the A293-sensitive K^+-current. I_{KCNK3} was strongly decreased (60%) in freshly isolated PASMCs from $Kcnk3^{\Delta 94ex1/+}$ rats and was abolished (95%) in $Kcnk3^{\Delta 94ex1/\Delta 94ex1}$ rats (Figure 1F and 1G). Consistent with the role of KCNK3 in resting membrane potential, PASMCs isolated from *Kcnk3*-mutated rats were significantly depolarized compared with PASMCs from WT rats (Figure 1H). We performed RT-qPCR (quantitative reverse transcription polymerase chain reaction) experiments to evaluate the consequences of *Kcnk3*-dysfunction on other lung K^+ channels (Online Figure III). No expression of KCNK4, KCNK9, $K_V1.4$, or $K_{Ca}4$ channels was detected. The mRNA expression levels of KCNK2, KCNK6, $K_V1.5$, $K_V2.1$, $K_V9.3$, $K_{Ca}1.1$, $K_{Ca}2.1$, $K_{Ca}2.2$, $K_{Ca}2.3$, and $K_{Ca}4.2$ was unchanged in *Kcnk3*-mutated rats compared with WT. However, we observed a significant increase in the mRNA level of $K_V1.2$ and $K_{Ca}3.1$ in $Kcnk3^{\Delta 94ex1/\Delta 94ex1}$ rat lungs. Yet, the A293-insensitive K^+-current was similar in PASMCs isolated from WT and *Kcnk3*-mutated rats (not shown), suggesting that *Kcnk3*-dysfunction is not compensated by other K^+ currents.

Kcnk3-Dysfunction Leads to an Increase in Right Ventricular Systolic Pressure in Males and Female

To determine whether *Kcnk3*-dysfunction leads to spontaneous PH, we performed closed chest right-heart catheterization at 4 months of age. We observed a slight but significant increase in right ventricular systolic pressure (RVSP) in $Kcnk3^{\Delta 94ex1/\Delta 94ex1}$ rats compared with WT

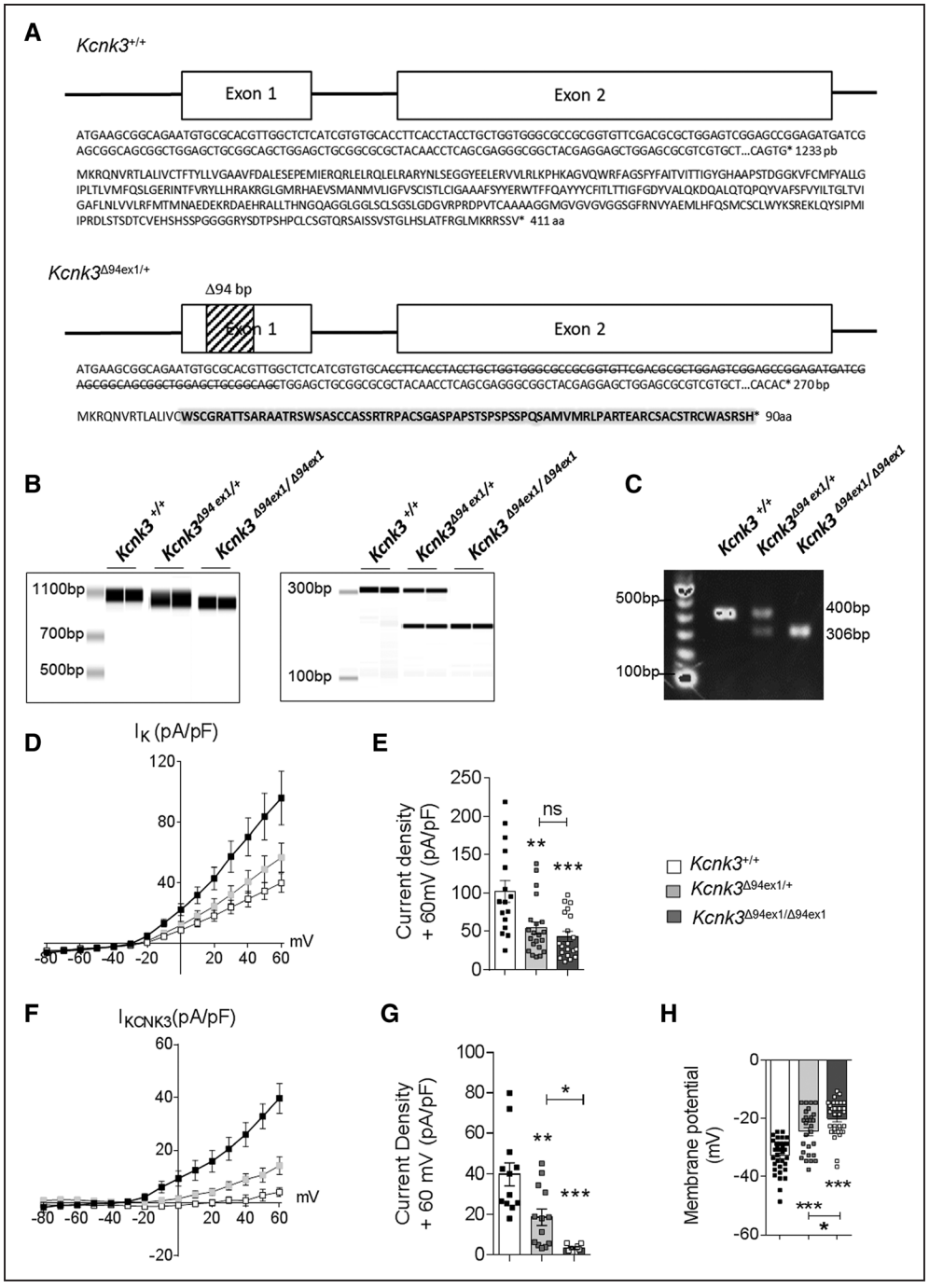

Figure 1. KCNK3 (potassium channel subfamily K member 3) is no longer functional in pulmonary arterial smooth muscle cells (PASMCs) from Kcnk3-mutated rats.

A, Schematic overview of the *Kcnk3* gene with wild-type (WT) and *Kcnk3*-mutant alleles. We generated *Kcnk3*-mutated rats with 94 bp deletion in exon 1 of the *Kcnk3* (Δ94ex1). Below, Kcnk3 DNA and Δ94 bp DNA (strikethrough letter) and protein sequences in WT and Δ94ex1 rats. Gray: aberrant/potential protein sequence. *STOP codon. **B**, mRNA levels of *Kcnk3* analyzed by RT-PCR (reverse transcription polymerase chain reaction) in $Kcnk3^{\Delta 94ex1/\Delta 94ex1}$ rats, $Kcnk3^{\Delta 94ex1/+}$ rats, and $Kcnk3^{+/+}$ rats, using 2 oligo combinations rKcnk3-17F/rKcnk3-1146R (left; WT: 1148 bp/Δ94ex1: 1054 bp) and rKcnk3-17F/rKcnk3-303R (right; WT: 304 bp/Δ94ex1: 210 bp). **C**, Validation of the deletion by PCR, showing genomic DNA amplicons from rats carrying the $Kcnk3^{+/+}$allele (400 bp) and Δ94ex1deletion allele (306 bp). **D**, Current-voltage relationship of global-K^+-currents, in freshly isolated PASMCs from $Kcnk3^{+/+}$, $Kcnk3^{\Delta 94ex1/+}$ and $Kcnk3^{\Delta 94ex1/\Delta 94ex1}$ rats, corresponding to the depolarizing step protocol (+60 mV to −100 mV, holding potential −40 mV). **E**, The current was normalized by the capacitance of the cell and is represented in pA/pF (pico ampere/pico farad; WT=16 cells, 4 rats, $Kcnk3^{\Delta 94Ex1/+}$=21 cells, 4 rats, $Kcnk3^{\Delta 94Ex1/\Delta 94Ex1}$=20 cells, 4 rats). After recording, the global-K^+-current, KCNK3 current was isolated by applying a specific inhibitor (200 nmol/L, A293). I_{KCNK3} (A293 sensitive-K^+-current) was then measured and presented in (**F**, WT=12 cells, 4 rats, $Kcnk3^{\Delta 94Ex1/+}$=10 cells, 4 rats, $Kcnk3^{\Delta 94Ex1/\Delta 94Ex1}$=13 cells, 4 rats). **G**, Current density of I_{KCNK3} measured at +60 mV. **H**, Using a current clamp, we measured the resting membrane potential of freshly isolated PASMCs (WT=34 cells, 4 rats, $Kcnk3^{\Delta 94Ex1/+}$=28 cells, 4 rats, $Kcnk3^{\Delta 94Ex1/\Delta 94Ex1}$=35 cells, 4 rats). *$P$<0.05, **$P$<0.01, ***$P$<0.001 vs $Kcnk3^{+/+}$. Experiments were analyzed using 1-way ANOVA followed by Tukey post hoc test for multiple comparisons. ns indicates nonsignificant.

in males (Figure 2A) and in females (Online Figure IVA). However, increased RVSP was not accompanied by RV hypertrophy (Fulton index) nor by a change in cardiac output or mean carotid artery pressures in males (Figure 2A) and in females (Online Figure IVA). Total pulmonary resistances (TPR) were significantly increased in *Kcnk3*$^{\Delta 94ex1/\Delta 94ex1}$ rats compared with WT males (Figure 2A) and females (Online Figure IVA).

Using echocardiography, we examined the consequences of *Kcnk3*-dysfunction at 4 months old (males) on cardiac function. Pulmonary artery acceleration time was significantly reduced in *Kcnk3*-mutated rats (Figure 2B), indicating a higher resistive PA profile. In addition, heart rate was significantly increased in *Kcnk3*$^{\Delta 94ex1/\Delta 94ex1}$ rats. We did not observe modification in the other parameters measured in *Kcnk3*-mutated rats (Online Table IV).

In mice, *Kcnk3* deletion causes primary hyperaldosteronism.[18] Conversely, in 4-month-old male *Kcnk3*$^{\Delta 94ex1/\Delta 94ex1}$, serum aldosterone concentration significantly decreased, whereas no variations were observed in female (Online Figure V).

Kcnk3-Mutated Rats Were More Susceptible to Monocrotaline (MCT)-or Chronic Hypoxia (CH)–Induced PH

As shown in Figure 2A, 4-month-old *Kcnk3*-mutated rats displayed a modest but significant increase in RVSP. Therefore, we exposed 4-month-old male and female rats to MCT (60 mg/kg). *Kcnk3*-dysfunction increased the severity of MCT-induced PH as demonstrated by higher RVSP in both males and females *Kcnk3*-mutated group, associated with higher TPR (Figure 2C; Online Figure IVB) with no modification of mean carotid artery pressure (not shown). These results demonstrate that *Kcnk3*-dysfunction sensitizes rats to develop PH under MCT-exposure.

In addition, male rats were exposed to CH (10% O_2 for 3 weeks). As shown in Figure 2D, *Kcnk3*-dysfunction increased the severity of CH-induced PH, as demonstrated by higher RVSP and TPR values in *Kcnk3*-mutated rats, compared with WT rats.

Kcnk3-Dysfunction Leads to Distal Pulmonary Vessel Neomuscularization and Increases Collagen Crosslinking

We analyzed muscularization of small pulmonary vessels (<30 µm) by immunostaining against α-SMA (α-smooth muscle actin, smooth-muscle marker) and VWF (Von Willebrand factor, endothelium marker; Figure 3A). *Kcnk3*-mutated rats presented a significantly decreased percentage of nonmuscularized vessels along with significantly increased numbers of muscularized vessels (Figure 3B). Moreover, the level of fibrillar collagen assembly was abnormally increased in pulmonary vessels from *Kcnk3*-mutated rats (Figure 3C).

The increase in RVSP in *Kcnk3*-mutated rats could also be explained by the modification of pulmonary microvessel density. By counting the number of CD31$^+$ (cluster of differentiation-31) pulmonary vessels, we did not detect modification of microvessel density in *Kcnk3*-mutated rats compared with WT (Figure 3D). However, Western blot analysis showed significant decreases of CD31 and significant increases of VWF expression in lungs from *Kcnk3*$^{\Delta 94ex1/\Delta 94ex1}$ rats (Figure 3E). Both molecules are critical to maintaining endothelial integrity, suggesting that *Kcnk3*-dysfunction may result in an alteration of the endothelial functions.

Proliferation Pathways Were Activated in Kcnk3-Mutated Rat Lungs

We analyzed the expression and activation of some proproliferative or antiapoptotic proteins known to contribute to PAH pathobiology. Compared with WT, the phosphorylation state of ERK 1/2, and SRC significantly increased in lung from *Kcnk3*-mutated rats, without modification of P38 (Figure 4A). We found that HIF1-α (hypoxia-inducible factor-1 α) expression was also significantly increased in lungs from *Kcnk3*-mutated rats (Figure 4A), without alteration of *HIF1-α* mRNA expression (not shown). We also measured an increase in the survivin protein in *Kcnk3*$^{\Delta 94ex1/\Delta 94ex1}$ rats (Figure 4A). AKT (protein kinase B) phosphorylation at Thr308 significantly increased in *Kcnk3*$^{\Delta 94ex1/\Delta 94ex1}$ rats (Figure 4A). ERK1/2 and AKT are targets for serine–threonine PP2A (protein phosphatase 2A). As presented in Online Figure VIA, the expression of PP2A-A, PP2A-B, and PP2A-C proteins was unchanged. However, we showed that PP2A phosphatase activity was strongly reduced (50%) in PASMCs from *Kcnk3*$^{\Delta 94ex1/\Delta 94ex1}$ compared with PASMCs from WT rats, while PP2B (or calcineurin) activity was unchanged (Figure 4B).

We also measured several other molecules known to be involved in PAH pathogenesis. We observed an increase in the expression of the endothelial-to-mesenchymal (endoMT) transcription factor TWIST1 (twist family bHLH transcription factor 1) and a decrease in the phosphorylation of CREB (cAMP response element–binding protein) in *Kcnk3*$^{\Delta 94ex1/\Delta 94ex1}$rats (Figure 4C), which are altered in PAH patients.[19,20] We measured an increase in the mRNA of *Nfatc1*, *Notch3*, *Mmp2*, and *Stat3* in *Kcnk3*$^{\Delta 94ex1/\Delta 94ex1}$ rats (Online Figure VIB). No variation for BMPRII, phospho-SMAD1/5/8, phospho-SMAD2/3, and Caveolin-1 protein expression was observed in lungs from *Kcnk3*-mutated rats (Online Figure VII).

The mRNA expression of *IL-6*, IL-6 receptor (*GP130*), *IL-17Ra* and *Timp1* was unchanged in the lung from *Kcnk3*-mutated rats at 4 months old (Online Figure VIIIA).

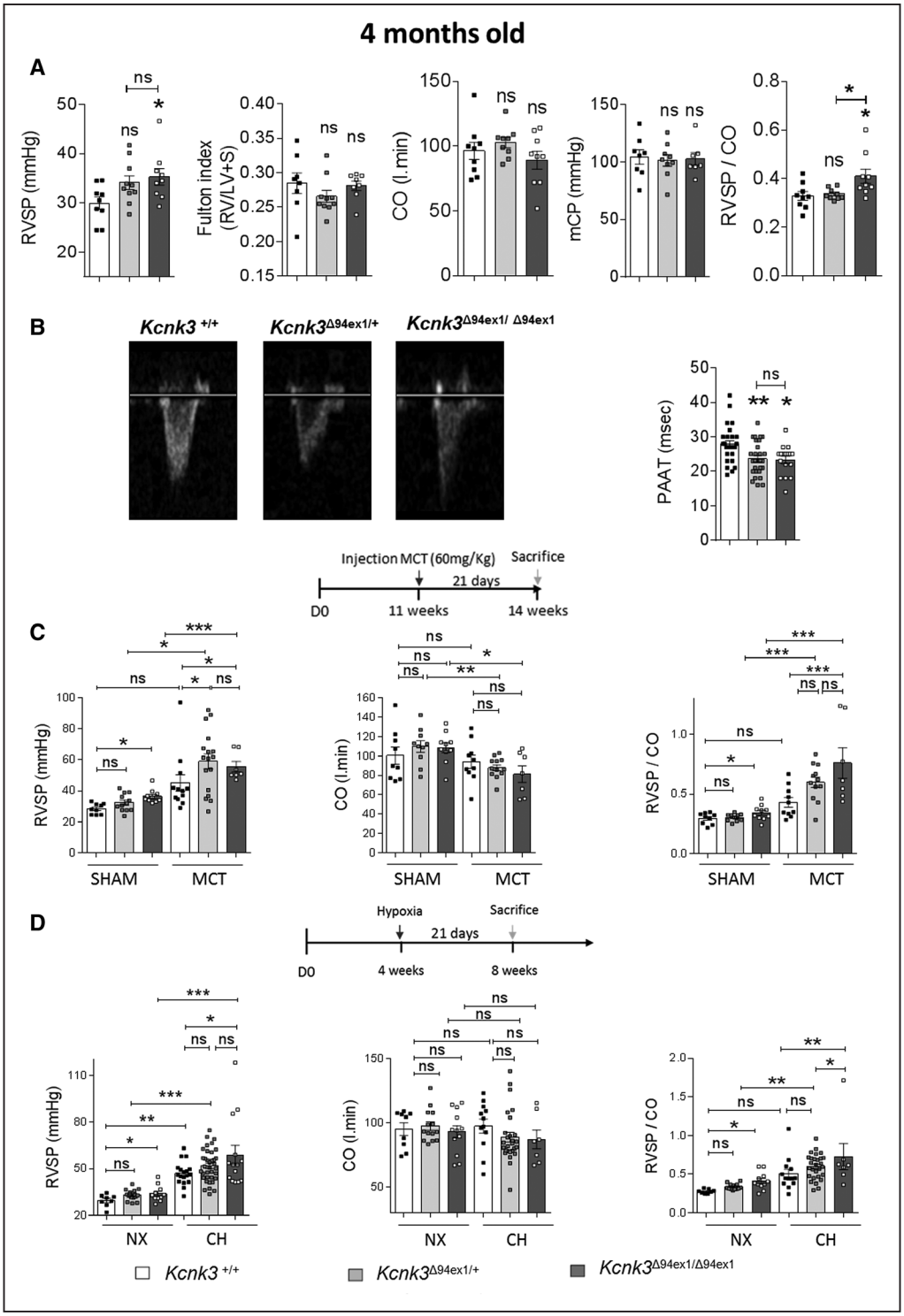

Figure 2. Kcnk3 (potassium channel subfamily K member 3) dysfunction leads to a significant increase in right ventricular systolic pressure (RVSP) in males at 4 months of age.

A, Quantification of right ventricular systolic pressure (RVSP), Fulton index (weight of right ventricle [RV]/left ventricle [LV]+septum [S]), cardiac output (CO), mean carotid pressure (mCP), and total pulmonary resistance (TPR evaluated by RVSP/CO; wild type [WT]=8 $Kcnk3^{\Delta 94Ex1/+}$=9, $Kcnk3^{\Delta 94Ex1/\Delta 94Ex1}$=9 rats). **B**, Representative pulmonary artery (PA) flow through the pulmonary valve in $Kcnk3^{+/+}$and *Kcnk3*-mutated rats and quantification of the PA acceleration time (PAAT; WT=26, $Kcnk3^{\Delta 94Ex1/+}$=29, $Kcnk3^{\Delta 94Ex1/\Delta 94Ex1}$=17rats). **C**, At 4-month old, male $Kcnk3^{+/+}$and *Kcnk3*-mutated rats were exposed to 60 mg/kg of monocrotaline (MCT) or saline (SHAM). Three weeks later, we measured RVSP, CO, and TPR (SHAM; WT=9, $Kcnk3^{\Delta 94Ex1/+}$=12, $Kcnk3^{\Delta 94Ex1/\Delta 94Ex1}$=10, MCT; WT=12, $Kcnk3^{\Delta 94Ex1/+}$=17, $Kcnk3^{\Delta 94Ex1/\Delta 94Ex1}$=7 rats). **D**, Four-month-old male $Kcnk3^{+/+}$and *Kcnk3*-mutated rats were exposed 3 weeks to chronic hypoxia (CH, 10% O_2) or normoxia (NX). Three weeks later, we measured RVSP, CO, and TPR (NX; WT=8, $Kcnk3^{\Delta 94Ex1/+}$=16, $Kcnk3^{\Delta 94Ex1/\Delta 94Ex1}$=11, CH; WT=18, $Kcnk3^{\Delta 94Ex1/+}$=36, $Kcnk3^{\Delta 94Ex1/\Delta 94Ex1}$=14 rats). *$P$<0.05, **$P$<0.01, ***$P$<0.001. Experiments were analyzed using 1-way ANOVA followed by Tukey post hoc test and experiments with 2 different categorical independent variables were analyzed with 2-way ANOVA completed by Tukey post hoc test for multiple comparisons. ns indicates nonsignificant.

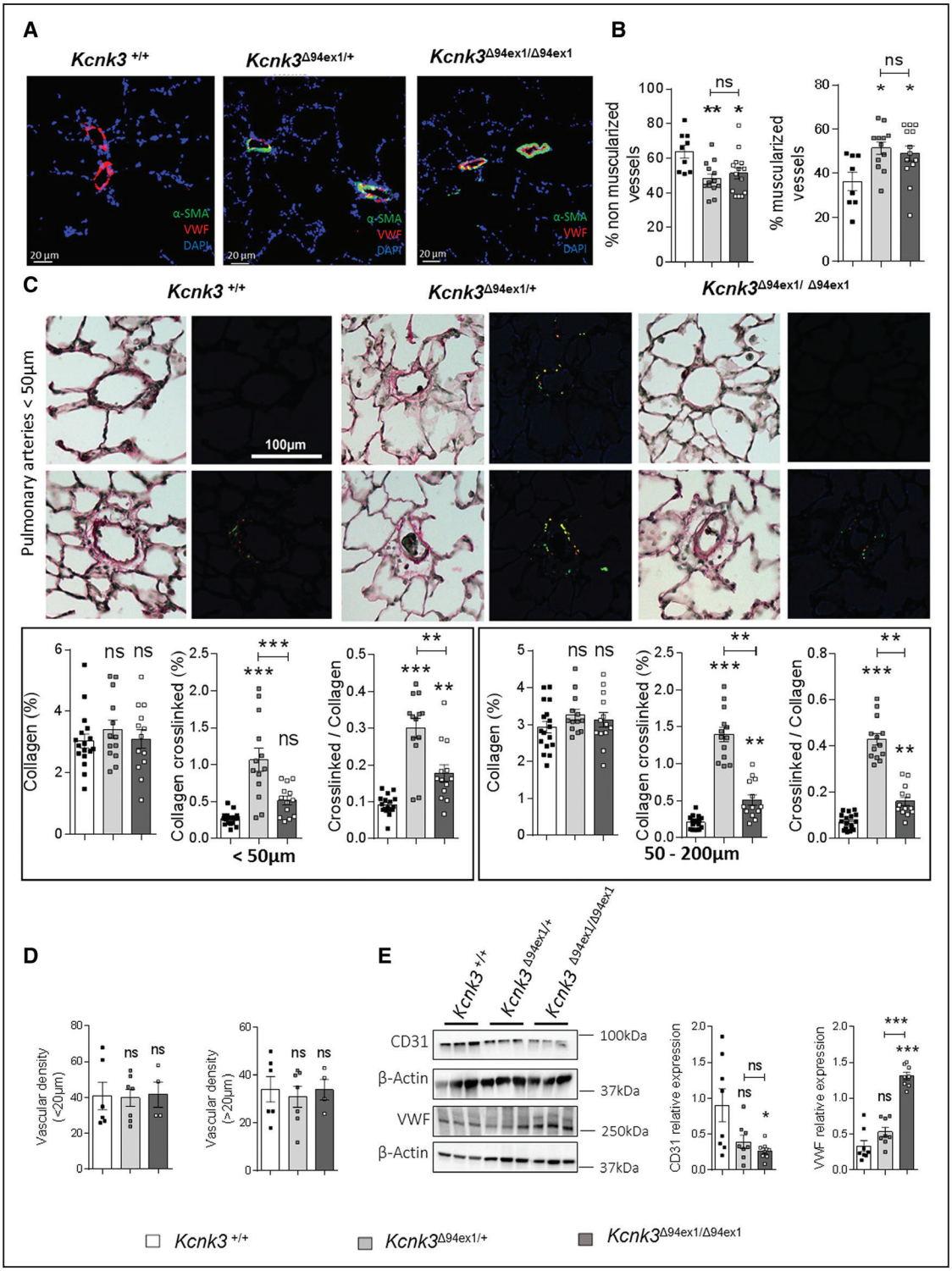

Figure 3. Kcnk3 (potassium channel subfamily K member 3)-dysfunction leads to distal pulmonary vessel neomuscularization and increased collagen crosslinking.

A, Immunolabeling and confocal imaging of α-SMA (α-smooth muscle actin) in green, VWF (Von Willebrand factor) in red, and DAPI in blue on rat lung sections. Scale bar: 20 µm. **B**, Percentage of nonmuscularized vessels and muscularized vessels (100 vessels counted per rat, wild type [WT]=9, *Kcnk3*$^{\Delta 94Ex1/+}$=13, *Kcnk3*$^{\Delta 94Ex1/\Delta 94Ex1}$ =14 rats). **C**, Upper, Picrosirius Red staining and below quantification of total collagen signal, collagen crosslinked, and crosslinked/collagen total ratio in small (<50 µm) and medium (50–200 µm) pulmonary artery from rats at 4 months old (WT=17, *Kcnk3*$^{\Delta 94Ex1/+}$=13, *Kcnk3*$^{\Delta 94Ex1/\Delta 94Ex1}$=13 rats). Scale bar: 100 µm. **D**, Pulmonary vessel density quantification based on CD31 (endothelium marker) labeling in paraffin-embedded lung sections, expressed as the percentage of small (<20 µm) or large (>20 µm) CD31$^+$ vessels measured in 20 fields of *Kcnk3*$^{+/+}$and *Kcnk3*-mutated rats at 4 months old (WT=6, *Kcnk3*$^{\Delta 94Ex1/+}$=7, *Kcnk3*$^{\Delta 94Ex1/\Delta 94Ex1}$=4 rats). **E**, Representative Western blots and quantification of CD31 and VWF expression in lungs from *Kcnk3*$^{+/+}$and *Kcnk3*-mutated rats (WT=8, *Kcnk3*$^{\Delta 94Ex1/+}$=8, *Kcnk3*$^{\Delta 94Ex1/\Delta 94Ex1}$=8 rats). β-actin was used as the loading control. . *P<0.05, **P<0.01, ***P<0.001 vs *Kcnk3*$^{+/+}$. Experiments were analyzed using 1-way ANOVA followed by Tukey post hoc test for multiple comparisons. ns indicates nonsignificant.

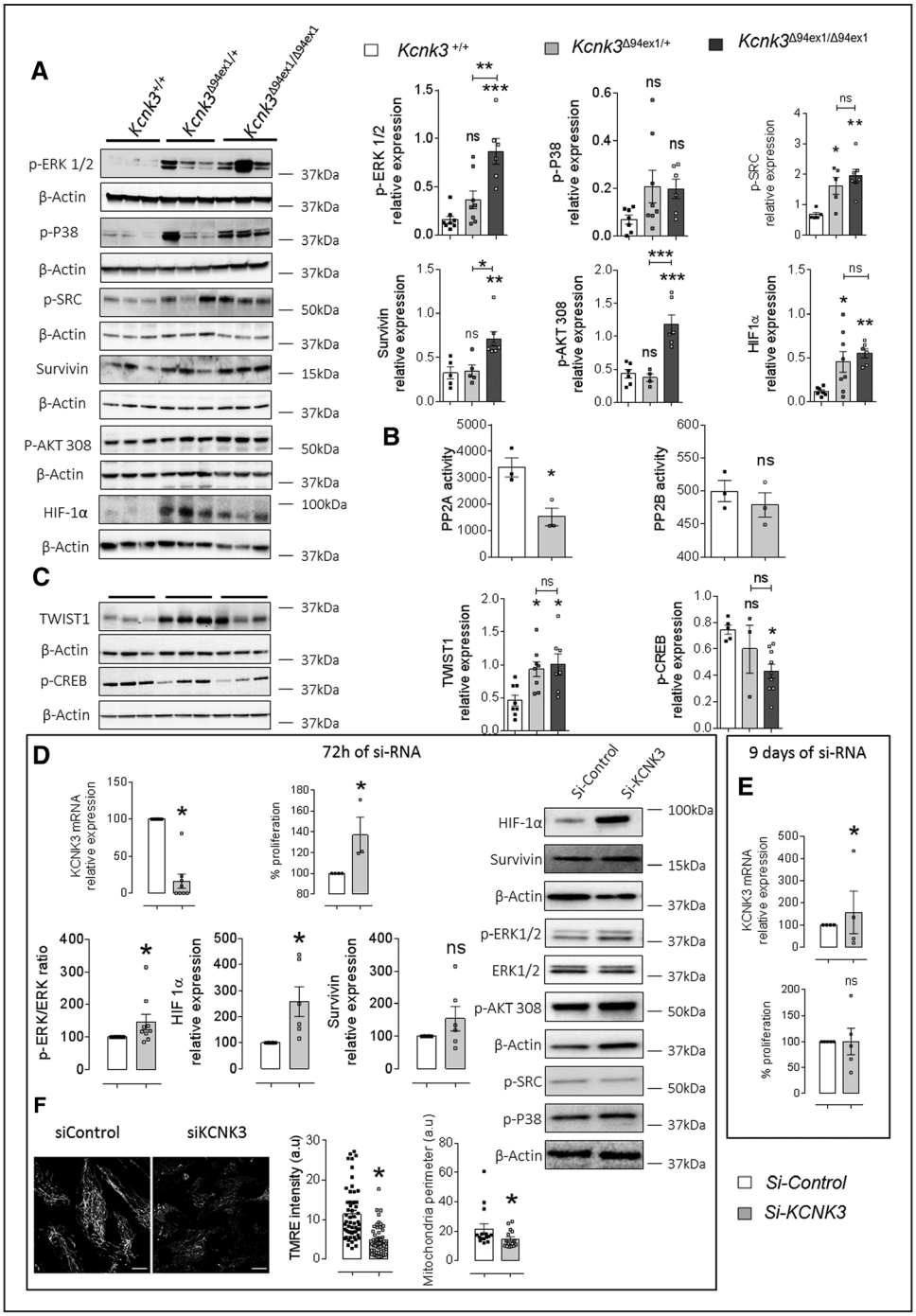

Figure 4. In vivo and in vitro Kcnk3 (potassium channel subfamily K member 3)-dysfunction leads to activation of several proproliferative and antiapoptotic pathways.

A, Representative Western blots and quantification of p-ERK1/2, p-P38, p-SRC, Survivin, HIF1-α (hypoxia-inducible factor-1 α), and p-308 AKT (protein kinase B) expression in lungs from wild-type (WT) and *Kcnk3*-mutated rats (WT=7, $Kcnk3^{\Delta 94Ex1/+}$=8, $Kcnk3^{\Delta 94Ex1/\Delta 94Ex1}$=6 rats). **B**, Quantification of PP2A and PP2B activity in pulmonary arterial smooth muscle cells (PASMCs) from WT and $Kcnk3^{\Delta 94ex1/\Delta 9e4x1}$ (WT=3, $Kcnk3^{\Delta 94Ex1/\Delta 94Ex1}$=3rats). **C**, Representative Western blots and quantification of TWIST1 (twist family bHLH transcription factor 1) and p-CREB expression in lungs from $Kcnk3^{+/+}$and *Kcnk3*-mutated rats (WT=8, $Kcnk3^{\Delta 94Ex1/+}$=8, $Kcnk3^{\Delta 94Ex1/\Delta 94Ex1}$ =7 rats). **D**, Upper: left, *KCNK3* mRNA level in human control PASMCs transfected 72 h with a si-RNA control (si-Control) or against KCNK3 (si-KCNK3; n=8patients), normalized by 18S mRNA expression. Right, percentage of proliferation of human PASMCs (hPASMCs) transfected with si-KCNK3 compared with Si-Control (n=6patients). **D**, Below: representative Western blots and quantifications of HIF1α, Survivin, p-ERK 1/2, ERK 1/2, p-AKT308, p-SRC, and p-P38 in hPASMCs, 72 h after si-RNA transfection. **E**, Upper, KCNK3 mRNA level in human control PASMCs, 9 days after cell transfection with si-RNA (n=4 patients), normalized by *18S* mRNA expression. Below, percentage of si-KCNK3 hPASMC proliferation compared with si-Control (n=4patients). **F**, confocal imaging of mitochondrial membrane potential (Δφm) using TMRE (Tetramethylrhodamine, ethyl ester) on hPASMCs treated with si-RNA. Right, quantification of TMRE intensity and mitochondria perimeter. ns: nonsignificant. *P<0.05, **P<0.01 vs $Kcnk3^{+/+}$or si-Control. Experiments were analyzed using 2-tailed unpaired Student test. ERK1/2 indicates extracellular signal–regulated kinase1-/2.

Likewise, the lung expression of CD45 (pan-leukocyte marker) was also unchanged (Online Figure VIIIB).

In Vitro KCNK3 Knockdown or Pharmacological KCNK3 Inhibition Increases Human PASMCs Proliferation

To evaluate the role of KCNK3 in human PASMCs (hPASMCs) and human pulmonary arterial endothelial cells proliferation, we abolished KCNK3 function using either si-RNA-mediated or specific pharmacological inhibition. Seventy two hours after transfection, *KCNK3* mRNA decreased in hPASMCs transfected with si-KCNK3 (by 85%). KCNK3 knockdown enhanced hPASMCs proliferation by 40% as measured by BrdU incorporation (Figure 4D). Pharmacological inhibition of KCNK3 by 24-hour exposure to A293 at 1 µmol/L enhances the proliferation of control PASMCs from humans and rats (Online Figure IXA).

In human pulmonary arterial endothelial cells exposed to the KCNK3 inhibitor, we observed significantly decreased proliferation rate compared with the vehicle condition (Online Figure IXC). Using iCelligence™, we observed that specific KCNK3 inhibition enhances human pulmonary arterial endothelial cells adhesion without alteration of endothelial barrier opening by TNFα (tumor necrosis factor α) stimulation (5 ng/mL; Online Figure IXD and IXE).

Consistent to an enhancement of PASMCs proliferation by the knockdown of KCNK3, we found a significant increase in the expression of HIF1-α, an over-phosphorylation of ERK1/2, and a nonsignificant increase of survivin, without modification of P38, SRC, and AKT phosphorylation (Figure 4D). Nine days after si-RNA transfection, *KCNK3* expression returned to the normal, hPASMCs proliferation was normalized (Figure 4E) as well as HIF1-α expression and ERK1/2 activation (Online Figure IXB), demonstrating that loss of KCNK3 enhances PASMCs proliferation. In addition to HIF1-α and ERK1/2 overactivation in si-KCNK3-treated hPASMCs, we found that mitochondria membrane were depolarized (TMRE fluorescence intensity, tetramethylrhodamine, ethyl ester) and fragmented compared with mitochondria from si-Control hPASMCs (Figure 4F), without modification of the total expression of the regulating mitochondrial fission protein DRP1 (dynamin related protein-1; Online Figure XA). Likewise, we found that the mitochondria of PASMCs from *Kcnk3*$^{\Delta 94ex1/\Delta 94ex1}$rats were also significantly depolarized and fragmented compared with WT. This strongly suggests that KCNK3 is involved in mitochondria integrity in human and rat PASMC (Online Figure XB and XC). We found that plasma membrane depolarization (induced by138 mM KCl) strongly depolarized mitochondria membrane without modification of mitochondrial web (Online Figure XD and XE).

Kcnk3-Dysfunction Predisposes PA to Constriction

We investigated the consequences of *Kcnk3*-dysfunction on PA contractility. Using isolated PA from 4-month-old WT and *Kcnk3*-mutated rats, we first assessed the consequence of *Kcnk3*-dysfunction on basal PA tone, measured as the extracellular Ca^{2+}-dependent tone. The basal tone was unaltered in *Kcnk3*-mutated rats (Online Figure XIA). The contractile dose-response to increasing doses of KCl was unchanged in PA from *Kcnk3*$^{\Delta 94ex1/+}$ compared with PA from WT rats whereas the dose-response curve of PA from *Kcnk3*$^{\Delta 94ex1/\Delta 94ex1}$ rats was significantly shifted to the left as shown by the significant decrease in EC_{50} (Figure 5A).

When PA were pretreated with Bay K 8644, a drug that potentiates voltage-sensitivity of L-Type-Ca^{2+} channels, the contractile response was shifted to the left compared with the condition without Bay K 8644 (Figure 5B). Importantly, L-Type Ca^{2+} channel potentiation abolished the previously observed differences in Figure 5A, consistent with the PASMCs depolarization (Figure 1H).

To rule out the contribution of endothelial-dependent PA relaxation via nitric oxide synthase (NOS) activities, we pretreated PA with L-NAME (L-N^G-nitroarginine methyl ester; NOS inhibitor). With L-NAME, PA contracted at a lower concentration of KCl than in the absence of L-NAME, demonstrating the contribution of NOS activities and validating the efficacy of L-NAME treatment (Figure 5C). Interestingly, with L-NAME, in *Kcnk3*$^{\Delta 94ex1/\Delta 94ex1}$ rats, the difference in the KCl contractile dose-response was lost (Figure 5C). Western blot analyses showed that endothelial-NOS expression was significantly reduced in lungs from *Kcnk3*$^{\Delta 94ex1/\Delta 94ex1}$ rats (Figure 5D), whereas inducible-NOS expression was unchanged (Online Figure XIB).

Pulmonary vascular endothelium also releases EDHF (endothelium-derived hyperpolarizing factor). EDHF represents a family of endothelial factors as an arachidonic acid metabolite produced by cytochrome P450-2C9 that hyperpolarize and relax smooth muscles. To investigate the contribution of EDHF in PA tone, we used fluconazole, a cytochrome P450 epoxygenase inhibitor. With fluconazole, WT PA contracted at a lower KCl concentration than in the basal condition (Figure 5E, left), whereas fluconazole had no impact on PA contraction in *Kcnk3*-mutated rats (Figure 5E, middle and right). These data suggested that EDHF production is strongly reduced or inefficient in *Kcnk3*-mutated rats. All these parameters (PASMCs depolarization, reduced endothelial-NOS expression, reduced EDHF sensitivity) may contribute to enhanced PA vasoconstriction in *Kcnk3*$^{\Delta 94ex1/\Delta 94ex1}$ rats.

Kcnk3-Dysfunction in Rats Reduced PA Relaxation

After inducing contraction with a thromboxane-A_2 mimetic (U46619), relaxation was stimulated using

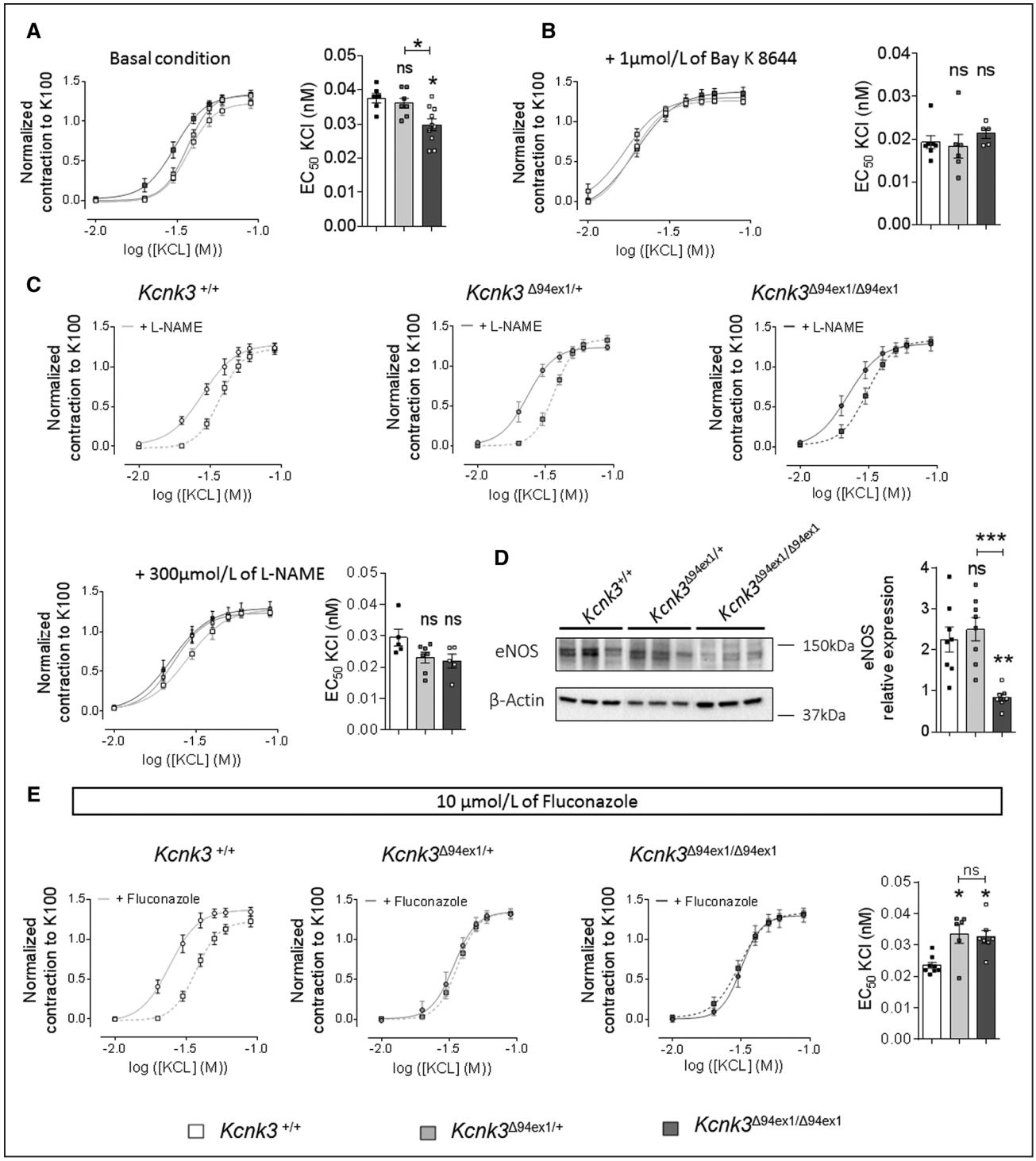

Figure 5. Kcnk3 (potassium channel subfamily K member 3)-dysfunction in rats predisposes pulmonary arteries to constriction. **A**, Normalized dose-response curve (normalized to K100) established by applying an increasing concentrations of KCl on isolated pulmonary artery (PA) from *Kcnk3*$^{+/+}$and *Kcnk3*-mutated rats and quantification of EC50 (WT=6, *Kcnk3*$^{\Delta 94Ex1/+}$=7, *Kcnk3*$^{\Delta 94Ex1/\Delta 94Ex1}$=10 rats). **B**, In presence of 1 µmol/L of Bay K 8644, normalized dose-response curve established by applying increasing concentrations of KCl on PA isolated from *Kcnk3*$^{+/+}$and *Kcnk3*-mutated rats and EC50 quantification (WT=7, *Kcnk3*$^{\Delta 94Ex1/+}$=6, *Kcnk3*$^{\Delta 94Ex1/\Delta 94Ex1}$=5 rats). **C**, Comparison of PA contraction, in response to increasing dose of KCl, between PA pretreated with 300 µmol/L of L-NAME (L-*N*^{G}-nitroarginine methyl ester) and PA nontreated (WT=5, *Kcnk3*$^{\Delta 94Ex1/+}$=7, *Kcnk3*$^{\Delta 94Ex1/\Delta 94Ex1}$=5 rats). Bottom, normalized dose-response curve established by applying increasing concentrations of KCl in the presence of 300 µmol/L of L-NAME and EC50 quantification (WT=5, *Kcnk3*$^{\Delta 94Ex1/+}$=7, *Kcnk3*$^{\Delta 94Ex1/\Delta 94Ex1}$=5 rats). **D**, Representative Western blots and quantification of eNOS expression in lungs from *Kcnk3*$^{+/+}$and *Kcnk3*-mutated rats (WT=8, *Kcnk3*$^{\Delta 94Ex1/+}$=8, *Kcnk3*$^{\Delta 94Ex1/\Delta 94Ex1}$=7 rats). β-actin was used as the loading control. **E**, Normalized dose-response curve established by applying increasing concentrations of KCl on isolated PA from *Kcnk3*$^{+/+}$and *Kcnk3*-mutated rats in presence of 10 µmol/L fluconazole and EC50 quantification (WT=8, *Kcnk3*$^{\Delta 94Ex1/+}$=6, *Kcnk3*$^{\Delta 94Ex1/\Delta 94Ex1}$=7 rats) . *$P$<0.05, **$P$<0.01 vs *Kcnk3*$^{+/+}$. Experiments were analyzed using 1-way ANOVA followed by Tukey post hoc test for multiple comparisons. ns indicates nonsignificant.

acetylcholine to induce endothelium-dependent relaxation, an NO donor (sodium nitroprusside [SNP]) to induce endothelium-independent relaxation and a PDE5 inhibitor (sildenafil; Figure 6). PA relaxation induced by acetylcholine or SNP was similar between WT and *Kcnk3*$^{\Delta 94ex1/+}$ rats, whereas significantly reduced in *Kcnk3*$^{\Delta 94ex1/\Delta 94ex1}$ rats (Figure 6A and 6B). Compared with WT, sildenafil-induced PA relaxation was reduced in *Kcnk3*-mutated rats, with a higher degree in *Kcnk3*$^{\Delta 94ex1/\Delta 94ex1}$ rats (Figure 6C), suggesting that KCNK3 is critical for PDE5 inhibition-mediated PA relaxation. To explore this hypothesis, we preincubated PA from WT rats with a KCNK3 inhibitor (A293, 1 µmol/L) and measured the sildenafil-induced relaxation. Sildenafil-mediated relaxation was reduced compared with vehicle condition (Figure 6D). The amount of PDE5A (Online Figure XIC) and its localization was similar in *Kcnk3*-mutated rats (not shown). These results suggest that KCNK3 is involved in the PDE5 inhibition-induced PA relaxation.

In addition, we found a gain of mRNA expression of various genes known to be involved in SMC phenotype switch, including *Hexim1*, *MYL6,* and *PLN* in isolated PA from *Kcnk3*$^{\Delta 94ex1/\Delta 94ex1}$ rats and decrease expression in *Hrpt1* in isolated PA from *Kcnk3*-mutated rats (Online Figure XID).

Kcnk3-Dysfunction Did Not Alter Both Constriction and Relaxation of Aorta or Pulmonary Veins

Interestingly, the contractile dose-response to KCl and the SNP-mediated relaxation were unchanged in aorta from *Kcnk3*-mutated rats (Online Figure XIIA and XIIB). Importantly, in isolated aorta, *Kcnk3*-dysfunction was not associated to an overactivation of MAP-kinase and antiapoptotic pathways (Online Figure XIIC). Finally, the contractile dose-response to KCl and the sildenafil-mediated relaxation in isolated pulmonary veins were unchanged in *Kcnk3*-mutated rats compared with WT (not shown), demonstrating specificity of the KCNK3 channel contribution in PAs. In line with normal aorta tone in *Kcnk3*-mutated rats, LV weights were similar in each group (Online Figure XIID and XIIE).

Kcnk3-Dysfunction Leads to Loss of Plasma Membrane Caveolae

Using electron microscopy imaging of PA, we found in *Kcnk3*$^{\Delta 94ex1/\Delta 94ex1}$ a decrease in the number of caveolae per micrometer localized into the luminal ECs surface compared with WT, while the total number of caveolae was unchanged (Figure 6E and 6F). Morphometric analysis of the depth of these caveolae invaginations in *Kcnk3*-mutated rats revealed that they were shallower than caveolae from WT pulmonary arterial endothelial cells (Figure 6F).

Kcnk3-Dysfunction Induces Action Potential Prolongation in RV Cardiomyocytes

In RV cardiomyocytes from *Kcnk3*-mutated rats, we recorded significant depolarization of resting membrane potential compared with WT (Figure 7A). Moreover, the action potentials were significantly prolonged in RV cardiomyocytes from *Kcnk3*$^{\Delta 94ex1/\Delta 94ex1}$ rats at −60 mV (Figure 7B). *Kcnk3*-mutated rats also showed some early after depolarization events (data not shown). Along with increased action potential duration, we measured a significant decrease in the outward-K^+-transient current (I_{to}; Figure 7C) and in an outward-K^+-sustained current (I_{sus}; Figure 7E). I_{to} was reduced without modification of inactivation time constants (data not shown). At mRNA level, we observed a significant decrease in the expression of Kv4.3 channels, while Kv4.2, Kv1.5, Kv1.2 expressions remained unchanged (Figure 7D and 7F). The background-inward-K^+-rectifier current (I_{K1}) was also strongly reduced in isolated RV cardiomyocytes from *Kcnk3*-mutated rats (Figure 7G), while KCNJ12 mRNA expression remained unchanged (Figure 7H). Together, these results demonstrate that KCNK3 contributes to RV cardiomyocyte excitability. The expression of *Atp2a2*, *Myh6,* and *Myh7* were also unchanged (Online Figure XIIIA). About RV inflammation in *Kcnk3*-mutated rats, we measured a significant increase of *Gp130* (IL-6 receptor component) and *Timp-1* mRNA in RV from *Kcnk3*$^{\Delta 94ex1/\Delta 94ex1}$ rats (Online Figure XIIIB).

Both Male and Female Kcnk3-Mutated Rats Developed an Age-Related Increase in RVSP (12 Months)

To determine whether PH development could be age-dependent, we performed right-heart catheterization in WT and *Kcnk3*-mutated rats at 12 months old (Figure 8A and Online Figure XIVA). PH is defined by an elevation of RVSP superior to 40 mm Hg. In males, RVSP was superior to 40 mmHg in 25% of *Kcnk3*$^{\Delta 94ex1/+}$ rats and in 45% of *Kcnk3*$^{\Delta 94ex1/\Delta 94ex1}$ rats associated with a significant increase in TPR (Figure 8A). In females, RVSP was superior to 40 mmHg in 20% of *Kcnk3*$^{\Delta 94ex1/+}$ rats and in 36% of *Kcnk3*$^{\Delta 94ex1/\Delta 94ex1}$ rats, associated with a significant increase in TPR (Online Figure XIVA).

In males and females, the elevation of RVSP was not associated with the development of RV hypertrophy (Fulton index) or a reduction in cardiac output (Figure 8A; Online Figures XIV and XV) nor alteration of mean carotid artery pressure values (Figure 8A; Online Figure XIVA).

In addition, we observed an increase in the number of muscularized pulmonary vessels and a decrease in nonmuscularized pulmonary vessels in 12-month-old male *Kcnk3*-mutated rats (Figure 8B) associated with HIF1-α overexpression in lung from *Kcnk3*$^{\Delta 94ex1/\Delta 94ex1}$ rats (Online Figure XIVB). Significant higher level of fibrillary

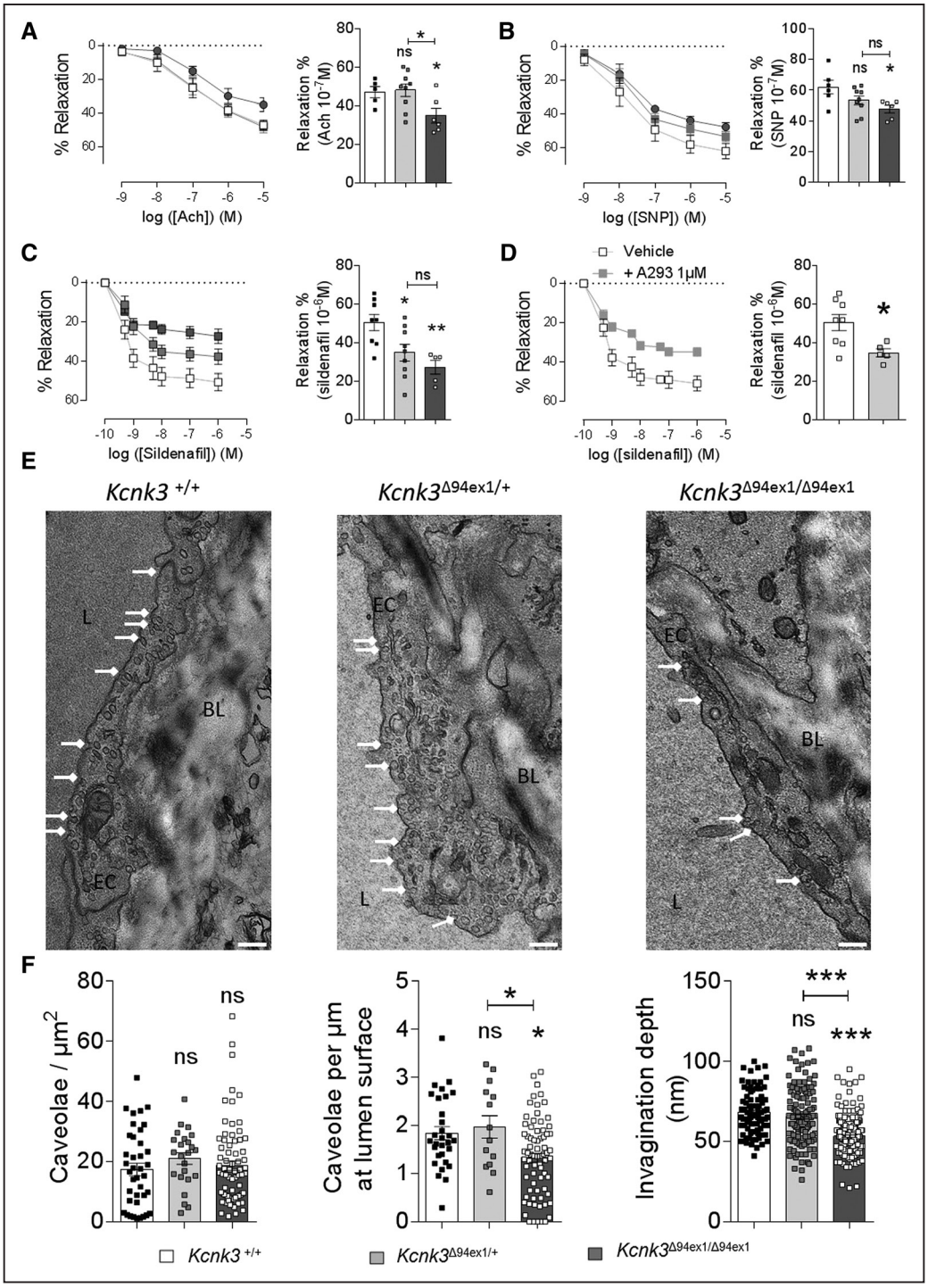

Figure 6. Kcnk3 (potassium channel subfamily K member 3)-dysfunction in rats altered the relaxation of pulmonary artery (PA). **A**, Concentration-relaxation response curves of isolated segment of PA established by applying increasing concentrations of (**A**) acetylcholine (Ach; 1 nmol/L to 10 µmol/L), (**B**) sodium nitroprusside (SNP; 10 nmol/L to 10 µmol/L) and (**C**) sildenafil (1 nmol/L to 5 µmol/L). Right, represent graph of the percentage of relaxation (WT=5, $Kcnk3^{\Delta 94Ex1/+}$=9, $Kcnk3^{\Delta 94Ex1/\Delta 94Ex1}$=7 rats). **D**, Concentration-relaxation response curves established by applying increasing concentrations of sildenafil (1 nmol/L to 10 µmol/L) to PA segments isolated from $Kcnk3^{+/+}$rats, treated with or without KCNK3 inhibitor (A293 1 µmol/L), and percentage of relaxation to 10^{-6} M of sildenafil (WT=6, $Kcnk3^{\Delta 94Ex1/+}$=9, $Kcnk3^{\Delta 94Ex1/\Delta 94Ex1}$=6 rats). **E**, Analysis of the ultrastructure of PA by electron microscopy in 4-month-old rats. Endothelial cells (ECs) were based on the basal lamina (BL). **F**, Caveolae density was quantified as the number of caveolae by micrometer square of total EC surface (Left; WT=34 cells, 2 rats, $Kcnk3^{\Delta 94Ex1/+}$=29 cells, 2 rats, $Kcnk3^{\Delta 94Ex1/\Delta 94Ex1}$=73 cells, 3 rats). Caveolae were counted as omega-shaped membrane profiles open at the lumen surface (L) and normalized per micrometer; WT=34 cells, 2 rats, $Kcnk3^{\Delta 94Ex1/+}$=29 cells, 2 rats, $Kcnk3^{\Delta 94Ex1/\Delta 94Ex1}$=73 cells, 3 rats; middle). Depths of the lumen caveolae (invagination depths) were quantified in right (WT=86 caveolae, 2 rats, $Kcnk3^{\Delta 94Ex1/+}$=131 caveolae, 2 rats, $Kcnk3^{\Delta 94Ex1/\Delta 94Ex1}$=234 caveolae, 3 rats). Bars= 400 nm. ns: nonsignificant. *P<0.05 **P<0.01, ***P<0.001 vs $Kcnk3^{+/+}$. Experiments were analyzed using 1-way ANOVA followed by Tukey post hoc test for multiple comparisons.

collagen assembly was observed in small (<50 µm) and medium (50–200 µm) PA in *Kcnk3*-mutated rats (Figure 8C), while total collagen deposition was similar (Online Figure XIVC).

At 12-month-old rats (males), echocardiography analyses (Online Table V) revealed a reduction in pulmonary artery acceleration time in *Kcnk3*-mutated rats. LV diastolic and systolic diameters (normalized by weight) significantly increased in *Kcnk3*-mutated rats along with reduction in RV and LV thickness, demonstrating development of LV dilatation in $Kcnk3^{\Delta 94ex1/\Delta 94ex1}$. LV dilatation seems to be compensated by higher RV and LV contractility as evaluated by RV and LV fractional shortening. At 12 months of age, *Kcnk3*-mutated rats showed chronic echography signs of left and right heart dilatation.

As low serum-albumin concentrations was associated with high mortality in PAH patients, serum-albumin was proposed as a marker of disease severity.[21] Interestingly, the serum-albumin level was unchanged in 4-month-old *Kcnk3*-mutated rats (Online Figure XIVD) but was significantly reduced in 12-month *Kcnk3*-mutated rats (Figure 8D), supporting the notion of age-dependent PH development in these animals.

DISCUSSION

In this study, we performed electrophysiological, hemodynamic, histological, cellular, and molecular characterization of *Kcnk3*-mutated rat line (Δ94ex1). First, we succeeded in generating a model of *Kcnk3*-inactivation with a decrease in I_{KCNK3} in PASMCs from *Kcnk3*-mutated rats. Second, at 4 months of age, RVSP are increased in *Kcnk3*-mutated rats and they are sensitized to PH induce by MCT-exposure or CH-exposure. Third, *Kcnk3*-dysfunction leads to increased pulmonary vessel muscularization and perivascular fibrillar collagen deposition. At the molecular level, *Kcnk3*-mutated rats are characterized by overactivation of proproliferative pathways, with alteration of endothelial marker expression. Fourth, in human PASMCs, KCNK3 knockdown increase the amount of HIF1-α and overactivate ERK1/2 pathway as primary molecular events linked to *Kcnk3*-dysfunction. Fifth, PAs from *Kcnk3*-mutated rats are sensitized to constriction and are less responsive to vasorelaxing stimuli. Finally, *Kcnk3*-mutated rats develop spontaneous PH in an age-dependent manner with penetrance ranging between 30% and 60%. The variety of pulmonary vascular alterations observed in *Kcnk3*-mutated rats are summarized in Figure 8E is consistent with recent findings related to human PAH pathobiology.[3]

KCNK3 channels are commonly accepted as contributors to background-K^+-currents that stabilize resting membrane potential.[8] In excitable cells including PASMCs, plasma membrane depolarization causes opening of L-type Ca^{2+} channels leading to influx of Ca^{2+}, PASMCs contraction, and proliferation via activation of Ca^{2+} sensitive pathways.[22] KCNK3 knockdown in mouse neuroblastoma cells increases proliferation rates by >25%.[23] In vivo chronic inhibition of KCNK3 induces aberrant pulmonary vascular cell proliferation.[10] We present evidence that pharmacological or genetic inactivation of KCNK3 promotes PASMCs proliferation, confirming that KCNK3 downregulation is an initial trigger for PAH pathobiology possibly via HIF1-α and ERK1/2 activation. In mice, *hif1-α*-dysfunction reduces the development of PH after CH-exposure.[24] In PAH, there is normoxic activation of HIF1-α inducing a pseudo-hypoxic cell status leading to aberrant cell proliferation,[25] which might be mediated by an activation of specific kinases (like P38 or ERK1/2)[26,27] or phosphatases inactivation.[26] We found that *Kcnk3*-dysfunction leads to overactivation of ERK1/2, which could partly enhance HIF1-α expression. Mitochondrial membrane depolarization induced by the mitochondrial uncoupler (FCCP [carbonyl cyanide-4(trifluoromethoxy)phenylhydrazone]) leads to the activation of ERK1/2.[28] Moreover, the resting plasma membrane potential and $\Delta\Psi m$ are intimately linked.[29] We found that extracellular high-K^+ concentration as well as si-KCNK3 induces mitochondrial membrane depolarization, which could also partly explain HIF1-α overexpression. Furthermore, mitochondrial dysfunction has been investigated in PAH, demonstrating that $\Delta\Psi m$ from PAH PASMCs are more hyperpolarized compared with mitochondria from healthy PASMCs because of an alteration of SOD2 expression.[30] However, SOD2 protein expression was unchanged in *Kcnk3*-mutated rats (not shown). Finally, previous reports demonstrated that mitochondrial network is fragmented in iPAH PASMCs[19] in association with the development of PAH. Here, we also found that mitochondria network is fragmented in the context of *Kcnk3*-dysfunction.

Our results suggest that *Kcnk3*-dysfunction enhances the phosphorylation of pro-mitogen proteins ERK1/2, 308AKT, and SRC and decreases PP2A activity. Indeed, we recently showed in iPAH PASMCs that T-type-Ca^{2+} channels signaling contributes to pathological hyperproliferation/cell survival and apoptosis resistance via phosphorylation of ERK1/2, 308AKT, and decreased PP2A activity.[31]

Higher levels of lung VWF have been associated with poor survival in PAH patients.[32] Mojiri et al[33] demonstrated that CH-exposure induced elevated lung VWF expression. We found that VWF expression is also severely increased in lung of *Kcnk3*-mutated rats, suggesting that *Kcnk3*-dysfunction alter also pulmonary endothelial function. CD31 is highly expressed at endothelial cell-cell junctions.[34] Here, we showed a decrease in CD31 expression in lungs from *Kcnk3*-mutated rats. Migrating endothelial cells lose specific endothelial markers such as CD31.[35] Increasing evidence demonstrates that EndMT contributes to PAH development.[20] EndMT is a process by which endothelial cells

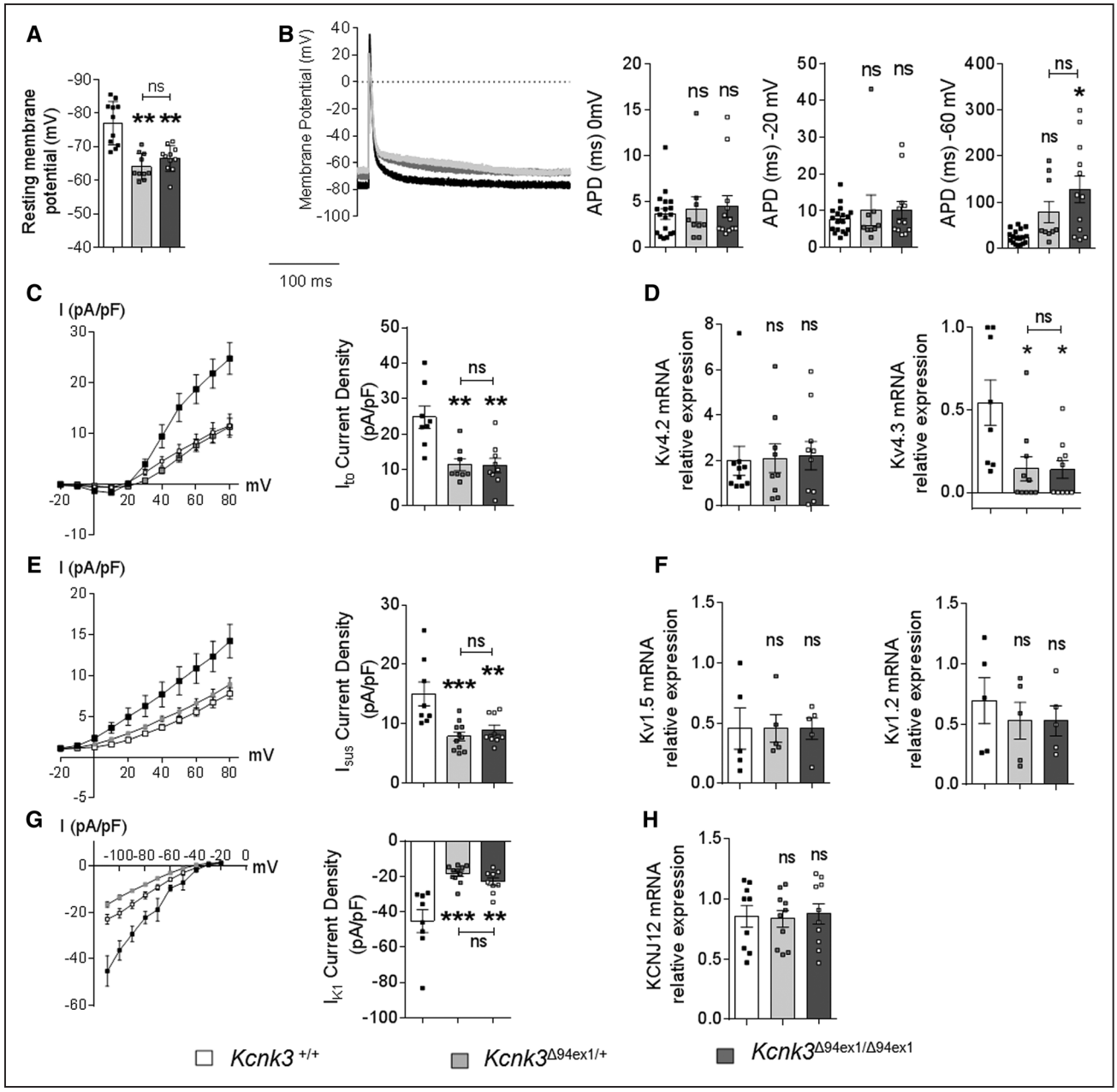

Figure 7. Kcnk3 (potassium channel subfamily K member 3)-dysfunction leads to action potential prolongation in adult right ventricular (RV) cardiomyocytes.

A, Average resting membrane potential in RV cardiomyocytes isolated from *Kcnk3*$^{+/+}$and *Kcnk3*-mutated rats (wild-type [WT]=11 cells, 3 rats, *Kcnk3*$^{\Delta 94Ex1/+}$=11 cells, 3 rats, *Kcnk3*$^{\Delta 94Ex1/\Delta 94Ex1}$=11 cells, 3 rats). **B**, Representative membrane potential of RV cardiomyocytes from *Kcnk3*$^{+/+}$and *Kcnk3*-mutated rats and analysis of RV action potential duration (APD) at 0, −20, and −60 mV of membrane repolarization (WT=20 cells, 4 rats, *Kcnk3*$^{\Delta 94Ex1/+}$=11 cells, 3 rats, *Kcnk3*$^{\Delta 94Ex1/\Delta 94Ex1}$=11 cells, 3 rats). **C**, We analyzed the current-voltage relationship of the outward-K^+-transient current (I_{to}) or 4-AP-sensitive-K^+ current (WT=8 cells, 3 rats, *Kcnk3*$^{\Delta 94Ex1/+}$=8 cells, 3 rats, *Kcnk3*$^{\Delta 94Ex1/\Delta 94Ex1}$=9 cells, 3 rats). **D**, mRNA expression of Kv4.2 and Kv4.3 in RV tissues (WT=11, *Kcnk3*$^{\Delta 94Ex1/+}$=11, *Kcnk3*$^{\Delta 94Ex1/\Delta 94Ex1}$=11 rats). **E**, Outward-sustained-K^+-current (I_{sus}) current (WT=11 cells, 3 rats, *Kcnk3*$^{\Delta 94Ex1/+}$=11 cells, 3 rats, *Kcnk3*$^{\Delta 94Ex1/\Delta 94Ex1}$=11 cells, 3 rats). **F**, mRNA expression of Kv1.5 and Kv2.1 in RV tissues from *Kcnk3*$^{+/+}$and *Kcnk3*-mutated rats (WT=5, *Kcnk3*$^{\Delta 94Ex1/+}$=5, *Kcnk3*$^{\Delta 94Ex1/\Delta 94Ex1}$=5 rats). **G**, Inward-$K^+$-rectifier-current ($I_{K1}$; WT=8 cells, 3 rats, *Kcnk3*$^{\Delta 94Ex1/+}$=11 cells, 3 rats, *Kcnk3*$^{\Delta 94Ex1/\Delta 94Ex1}$=9 cells, 3 rats). **H**, mRNA expression of KCNJ12 in RV tissues from *Kcnk3*$^{+/+}$and *Kcnk3*-mutated rats (WT=11, *Kcnk3*$^{\Delta 94Ex1/+}$=11, *Kcnk3*$^{\Delta 94Ex1/\Delta 94Ex1}$=11 rats). *$P$<0.05 vs *Kcnk3*$^{+/+}$. Experiments were analyzed using 1-way ANOVA followed by Tukey post hoc test for multiple comparisons. ns indicates nonsignificant.

acquire a mesenchymal phenotype in association with expression of SMC genes or loss of endothelial marker expression.[36] We showed an overexpression of TWIST1, mainly defined as a master controller of EndMT and epithelial-mesenchymal-transition,[20] suggesting *Kcnk3*-dysfunction contributes to EndMT pathway.

As caveolae are demonstrated to mediate albumin transcytosis in human ECs,[37] the loss of plasma-membrane

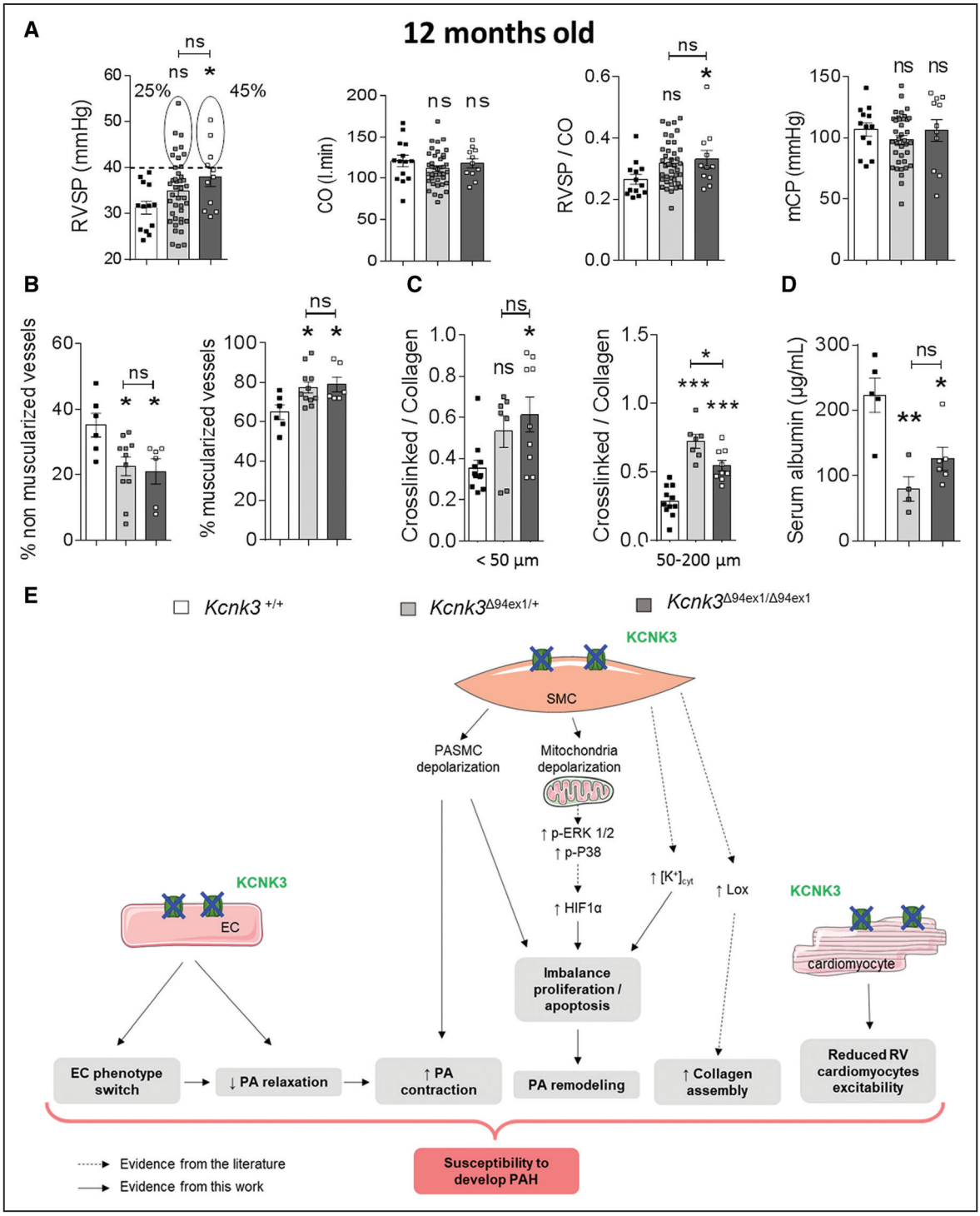

Figure 8. Kcnk3 (potassium channel subfamily K member 3)-mutated rats develop age-related pulmonary hypertension (12 mo). **A**, Right ventricular systolic pressure (RVSP), cardiac output (CO), total pulmonary resistance (TPR), and mean carotid pressure (mCP) were assessed at 12 months old (wild type [WT]=13, *Kcnk3*$^{\Delta 94Ex1/+}$=41, *Kcnk3*$^{\Delta 94Ex1/\Delta 94Ex1}$=11 rats). **B**, Percentage of nonmuscularized and muscularized vessels (100 vessels count per rats; WT=6, *Kcnk3*$^{\Delta 94Ex1/+}$=11, *Kcnk3*$^{\Delta 94Ex1/\Delta 94Ex1}$=6 rats). **C**, Collagen crosslinked to total collagen ratio in small (<50 µm) and medium (50–200 µm) pulmonary artery (PA) from *Kcnk3*$^{+/+}$and *Kcnk3*-mutated rats at 12 months old (WT=11, *Kcnk3*$^{\Delta 94Ex1/+}$=7, *Kcnk3*$^{\Delta 94Ex1/\Delta 94Ex1}$=9 rats). **D**, Serum-albumin concentration in plasma from *Kcnk3*$^{+/+}$and *Kcnk3*-mutated rats at 12 months old (WT=5, *Kcnk3*$^{\Delta 94Ex1/+}$=5, *Kcnk3*$^{\Delta 94Ex1/\Delta 94Ex1}$=6 rats). *$P$<0.05, **$P$<0.01 vs *Kcnk3*$^{+/+}$. Experiments were analyzed using 1-way ANOVA followed by Tukey post hoc test. **E**, Proposed events arising from *Kcnk3*-dysfunction. Loss of KCNK3 results in plasma membrane depolarization, mitochondrial membrane depolarization, endothelial phenotype switch, reduces RV cardiomyocytes excitability. All the events leads to pulmonary arterial vasoconstriction, pulmonary vascular remodeling, and pulmonary arterial smooth muscle cells (PASMCs) proliferation (partly explained by ERK1/2 increased phosphorylation and overexpression of HIF1-α [hypoxia-inducible factor-1 α]). Altogether, these events predispose for pulmonary vascular remodeling and pulmonary arterial hypertension (PAH). ns indicates nonsignificant.

caveolae in pulmonary arterial endothelial cells lacking KCNK3 could partly explain abnormal serum-albumin production in *Kcnk3*-mutated rats.

Moreover, increasing evidences suggest an important role of ECM (extracellular matrix) deposition in PAH. Numerous experimental PH models exhibit pulmonary vascular matrix deposition.[38] Interestingly at 4 months old, perivascular collagen cross-linking is markedly pronounced in heterozygous *Kcnk3*-mutated rats, which may contribute to abnormal RVSP elevation because perivascular collagen cross-linking is associated to PA stiffness.[3] Bertero et al[39] demonstrated in hPASMCs that the knockdown of KCNK3 promotes expression of the collagen crosslinking enzyme (lysyl oxidase) and promotes expression of miR130/301 that coordinate ECM remodeling.

In addition to PA remodeling and fibrosis, PAH patients have aberrant PA vasoconstricition mainly explained by the disruption of the NO pathway.[3] In PAH, endothelial-derived NO activity is decreased, promoting vasoconstriction and thrombosis.[40] As caveolae are shown to regulate endothelial-NOS activity,[41] the abnormalities observed in caveolae shape from pulmonary arterial endothelial cell *Kcnk3*-mutated rats could contribute to the decrease in NOS-mediated relaxation. Although EDHF is important to maintain normal vascular tone, the exact role of EDHF in PH pathogenesis is unclear. Alteration of EDHF-mediated responses has been reported with aging, hypertension, atherosclerosis, heart failure, and diabetes mellitus.[42] We showed that *Kcnk3*-dysfunction predisposes to PA vasoconstriction associated with reduced endothelial-NOS expression and alteration of EDHF pathway. Ouyang et al[43] have suggested that K^+-channels regulate NO secretion in human pulmonary arterial endothelial cells.[43] Our results strongly suggest a crosslink between KCNK3 and NO or EDHF in PA.

We found that PA relaxation, induced by PDE5 inhibition, is reduced when KCNK3 is not functional. PDE5 inhibition increase intracellular levels of cGMP, thus increasing PKG activity and consequently relaxing smooth muscles.[44] KCNK3 contains multiple PKG phosphorylation sites. As PKG regulates KCNK3 activity,[45] we propose that KCNK3 channel is the end point of PDE5/GMP/PKG dependent signaling in PASMCs.

At cardiac level, we confirmed that KCNK3 contributes to RV cardiomyocyte excitability and action potential repolarization. Moreover, we recently demonstrated that pharmacological inhibition of KCNK3 (by A293) increased the action potential duration in adult RV cardiomyocytes from rats.[11] Previous reports showed similar results in *kcnk3*-knockout mice.[46] In human iPSC (induced pluripotent stem cells)-derived cardiomyocytes, *KCNK3* knockdown was found to prolong action potential duration.[47] *Kcnk3*-dysfunction should increase the susceptibility for early after-depolarizations and ventricular arrhythmias.

Collectively, our findings, summarized in Figure 8E, underscore the concept that genetic *Kcnk3*-inactivation in rats leads to pulmonary vascular alteration, thus facilitating PH development in an age-dependent manner. Importantly, our results highlight that loss of KCNK3 function acts on PA compliance resulting in increased RVSP via 2 different ways. Heterozygous-*Kcnk3*$^{\Delta 94ex1/+}$ rats were characterized by PA remodeling and perivascular collagen crosslinking whereas PA remodeling and PA vasoconstriction (Online Figure XVI) characterize homozygous-*Kcnk3*$^{\Delta 94ex1/\Delta 94ex1}$ rats. These results confirm the importance of PA tone and mechanical cues at the early stages of PH development. This model provides new opportunities for understanding the initiating mechanisms of PH and represents a relevant tool for testing therapeutic targets against PH.

Limitations

Our *Kcnk3*-mutated rats cannot be considered as knockout animals. Using CRISPR/Cas9 approach, we induced a deletion of 94 bp in the exon 1 of *Kcnk3* gene, shifting the open reading frame. This shift in the coding sequence results in an aberrant aa sequence and leads to a premature stop codon (8 potential premature stop codons; Online Figure I. Unfortunately, commercially available KCNK3 antibodies are not specific to KCNK3 preventing any evaluation of the expression of WT or truncated KCNK3 proteins. The putative translation of the truncated mRNA should produce a 90-aa protein (instead of a 411-aa for the WT protein) with only 14-aa in common with the WT protein, which could partly affect a signaling cascade induced by *Kcnk3*-mutation. However, we show that most of KCNK3-dependent signaling observed in *Kcnk3*-mutated rats were also detected in hPASMC in which KCNK3 is targeted by siRNA strategy. These similar results (ex vivo versus in vivo) indicate that the truncated protein negligibly affected the *Kcnk3*-mutated phenotype.

ARTICLE INFORMATION

Received February 1, 2019; revision received July 17, 2019; accepted July 24, 2019.

Affiliations

From the University Paris–Sud, Faculté de Médecine, Université Paris-Saclay, Le Kremlin Bicêtre, France (M.L., V.C., A.B., M.K.N., A.H., C.R.-M., O.M., B.G., D.M., F.P., M. H., F.A.); Assistance Publique Hôpitaux de Paris, Service de Pneumologie, Centre de Référence de l'Hypertension Pulmonaire, Hôpital Bicêtre, Le Kremlin Bicêtre, France (M.L., V.C., A.B., M.K.N., A.H., C.R.-M., O.M., B.G., D.M., F.P., M.H., F.A.); Inserm UMR_S 999, Hôpital Marie Lannelongue, Le Plessis Robinson, France (M.L., V.C., A.B., M.K.N., A.H., C.R.-M., O.M., B.G., D.M., F.P., M.H., F.A.); Université Côte d'Azur, CNRS, IPMC, Valbonne, France (T.B.); Centre de Recherche en Transplantation et Immunologie UMR 1064, INSERM, Université de Nantes, France (L.T., S.R., I.A.); PTransgenic Rat ImmunoPhenomic (TRIP) facility Nantes, Nantes, France (L.T., S.R., I.A.); GABI, INRA, AgroParisTech, Université Paris-Saclay, 78350 Jouy-en-Josas, France (C.P.); Signalisation et Physiopathologie Cardiovasculaire - UMR_S 1180, Univ. Paris-Sud, INSERM, Université Paris-Saclay, Châtenay-Malabry, France (B.M.); Animal Facility, Institut Paris Saclay d'Innovation Thérapeutique (UMS IPSIT), Université Paris-Sud, Université Paris-Saclay, Châtenay-Malabry, France (V.D.); and Centre de Recherche de l'Institut Universitaire de Cardiologie et de Pneumologie de Québec, Laval University, Canada (F.P.).

Acknowledgments

This work benefited from the facilities and expertise of TEFOR—Investissement d'avenir—ANR-II-INSBS-0014. We wish to thank the staff at the ANIMEX platform for caring for the rat lines.

Sources of Funding

F. Antigny receives funding from the Fondation du Souffle et Fonds de Dotation Recherche en Santé Respiratoire from the Fondation Lefoulon-Delalande and from the Fondation Legs Poix. He also received funding from the National Funding Agency for Research: ANR-18-CE14-0023. F. Perros received funding from Fondation maladies rares in the frame of the small-animal models and rare diseases program to generate the *Kcnk3*-mutant rats. M. Lambert is supported by Therapeutic Innovation Doctoral School (ED569).

Disclosures

M. Humbert has relationships with drug companies, including Actelion, Bayer, GSK, Novartis, and Pfizer. In addition to being investigators in trials involving these companies, other relationships include consultancy services and memberships to scientific advisory boards. The other authors report no conflicts of interest.

REFERENCES

1. Lau EMT, Giannoulatou E, Celermajer DS, Humbert M. Epidemiology and treatment of pulmonary arterial hypertension. *Nat Rev Cardiol*. 2017;14:603–614. doi: 10.1038/nrcardio.2017.84
2. Simonneau G, Montani D, Celermajer DS, Denton CP, Gatzoulis MA, Krowka M, Williams PG, Souza R. Haemodynamic definitions and updated clinical classification of pulmonary hypertension. *Eur Respir J*. 2019;53:1801913.
3. Humbert M, Guignabert C, Bonnet S, Dorfmüller P, Klinger JR, Nicolls MR, Olschewski AJ, Pullamsetti SS, Schermuly RT, Stenmark KR, et al. Pathology and pathobiology of pulmonary hypertension: state of the art and research perspectives. *Eur Respir J*. 2019;53:1801887.
4. Ma L, Roman-Campos D, Austin ED, Eyries M, Sampson KS, Soubrier F, Germain M, Trégouët D-A, Borczuk A, Rosenzweig EB, et al. A novel channelopathy in pulmonary arterial hypertension. *N Engl J Med*. 2013;369:351–361.
5. Navas Tejedor P, Tenorio Castaño J, Palomino Doza J, Arias Lajara P, Gordo Trujillo G, López Meseguer M, Román Broto A, Lapunzina Abadía P, Escribano Subía P. An homozygous mutation in KCNK3 is associated with an aggressive form of hereditary pulmonary arterial hypertension. *Clin Genet*. 2017;91:453–457. doi: 10.1111/cge.12869
6. Best DH, Sumner KL, Smith BP, Damjanovich-Colmenares K, Nakayama I, Brown LM, Ha Y, Paul E, Morris A, Jama MA, et al. EIF2AK4 mutations in patients diagnosed with pulmonary arterial hypertension. *Chest*. 2017;151:821–828. doi: 10.1016/j.chest.2016.11.014
7. Higasa K, Ogawa A, Terao C, Shimizu M, Kosugi S, Yamada R, Date H, Matsubara H, Matsuda F. A burden of rare variants in BMPR2 and KCNK3 contributes to a risk of familial pulmonary arterial hypertension. *BMC Pulm Med*. 2017;17:57. doi: 10.1186/s12890-017-0400-z
8. Lambert M, Capuano V, Olschewski A, Sabourin J, Nagaraj C, Girerd B, Weatherald J, Humbert M, Antigny F. Ion channels in pulmonary hypertension: a therapeutic interest? *Int J Mol Sci*. 2018;19:E3162. doi: 10.3390/ijms19103162
9. Olschewski A, Veale EL, Nagy BM, Nagaraj C, Kwapiszewska G, Antigny F, Lambert M, Humbert M, Czirják G, Enyedi P, et al. TASK-1 (KCNK3) channels in the lung: from cell biology to clinical implications. *Eur Respir J*. 2017;50:1700754.
10. Antigny F, Hautefort A, Meloche J, Belacel-Ouari M, Manoury B, Rucker-Martin C, Péchoux C, Potus F, Nadeau V, Tremblay E, et al. Potassium channel subfamily K member 3 (KCNK3) contributes to the development of pulmonary arterial hypertension. *Circulation*. 2016;133:1371–1385. doi: 10.1161/CIRCULATIONAHA.115.020951
11. Lambert M, Boet A, Rucker-Martin C, Mendes-Ferreira P, Capuano V, Hatem S, Adão R, Brás-Silva C, Hautefort A, Michel JB, et al. Loss of KCNK3 is a hallmark of RV hypertrophy/dysfunction associated with pulmonary hypertension. *Cardiovasc Res*. 2018;114:880–893. doi: 10.1093/cvr/cvy016
12. Manoury B, Lamalle C, Oliveira R, Reid J, Gurney AM. Contractile and electrophysiological properties of pulmonary artery smooth muscle are not altered in TASK-1 knockout mice. *J Physiol*. 2011;589:3231–3246. doi: 10.1113/jphysiol.2011.206748
13. Pandit LM, Lloyd EE, Reynolds JO, Lawrence WS, Reynolds C, Wehrens XH, Bryan RM. TWIK-2 channel deficiency leads to pulmonary hypertension through a rho-kinase-mediated process. *Hypertension*. 2014;64:1260–1265. doi: 10.1161/HYPERTENSIONAHA.114.03406
14. Remy S, Chenouard V, Tesson L, Usal C, Ménoret S, Brusselle L, Heslan JM, Nguyen TH, Bellien J, Merot J, et al. Generation of gene-edited rats by delivery of CRISPR/Cas9 protein and donor DNA into intact zygotes using electroporation. *Sci Rep*. 2017;7:16554. doi: 10.1038/s41598-017-16328-y
15. Chang YF, Imam JS, Wilkinson MF. The nonsense-mediated decay RNA surveillance pathway. *Annu Rev Biochem*. 2007;76:51–74. doi: 10.1146/annurev.biochem.76.050106.093909
16. Schmidt C, Wiedmann F, Voigt N, Zhou XB, Heijman J, Lang S, Albert V, Kallenberger S, Ruhparwar A, Szabó G, et al. Upregulation of K(2P)3.1 K+ current causes action potential shortening in patients with chronic atrial fibrillation. *Circulation*. 2015;132:82–92. doi: 10.1161/CIRCULATIONAHA.114.012657
17. Murtaza G, Mermer P, Goldenberg A, Pfeil U, Paddenberg R, Weissmann N, Lochnit G, Kummer W. TASK-1 potassium channel is not critically involved in mediating hypoxic pulmonary vasoconstriction of murine intrapulmonary arteries. *PLoS One*. 2017;12:e0174071. doi: 10.1371/journal.pone.0174071
18. Davies LA, Hu C, Guagliardo NA, Sen N, Chen X, Talley EM, Carey RM, Bayliss DA, Barrett PQ. TASK channel deletion in mice causes primary hyperaldosteronism. *Proc Natl Acad Sci USA*. 2008;105:2203–2208. doi: 10.1073/pnas.0712000105
19. Hong Z, Chen KH, DasGupta A, Potus F, Dunham-Snary K, Bonnet S, Tian L, Fu J, Breuils-Bonnet S, Provencher S, et al. MicroRNA-138 and MicroRNA-25 down-regulate mitochondrial calcium uniporter, causing the pulmonary arterial hypertension cancer phenotype. *Am J Respir Crit Care Med*. 2017;195:515–529. doi: 10.1164/rccm.201604-0814OC
20. Ranchoux B, Antigny F, Rucker-Martin C, Hautefort A, Péchoux C, Bogaard HJ, Dorfmüller P, Remy S, Lecerf F, Planté S, et al. Endothelial-to-mesenchymal transition in pulmonary hypertension. *Circulation*. 2015;131:1006–1018. doi: 10.1161/CIRCULATIONAHA.114.008750
21. Snipelisky D, Jentzer J, Batal O, Dardari Z, Mathier M. Serum albumin concentration as an independent prognostic indicator in patients with pulmonary arterial hypertension. *Clin Cardiol*. 2018;41:782–787. doi: 10.1002/clc.22954
22. Boucherat O, Chabot S, Antigny F, Perros F, Provencher S, Bonnet S. Potassium channels in pulmonary arterial hypertension. *Eur Respir J*. 2015;46:1167–1177. doi: 10.1183/13993003.00798-2015
23. Hao X, Li X. The knockdown of TASK-1 channels improved the proliferation of N2A cells. *J Mol Neurosci*. 2015;55:314–317. doi: 10.1007/s12031-014-0323-6
24. Yu AY, Shimoda LA, Iyer NV, Huso DL, Sun X, McWilliams R, Beaty T, Sham JS, Wiener CM, Sylvester JT, et al. Impaired physiological responses to chronic hypoxia in mice partially deficient for hypoxia-inducible factor 1alpha. *J Clin Invest*. 1999;103:691–696. doi: 10.1172/JCI5912
25. Ryan JJ, Archer SL. Emerging concepts in the molecular basis of pulmonary arterial hypertension: part I: metabolic plasticity and mitochondrial dynamics in the pulmonary circulation and right ventricle in pulmonary arterial hypertension. *Circulation*. 2015;131:1691–1702. doi: 10.1161/CIRCULATIONAHA.114.006979
26. Ueda S, Masutani H, Nakamura H, Tanaka T, Ueno M, Yodoi J. Redox control of cell death. *Antioxid Redox Signal*. 2002;4:405–414. doi: 10.1089/15230860260196209
27. He X, Wang J, Wei W, Shi M, Xin B, Zhang T, Shen X. Hypoxia regulates ABCG2 activity through the activivation of ERK1/2/HIF-1α and contributes to chemoresistance in pancreatic cancer cells. *Cancer Biol Ther*. 2016;17:188–198. doi: 10.1080/15384047.2016.1139228
28. Luo Y, Bond JD, Ingram VM. Compromised mitochondrial function leads to increased cytosolic calcium and to activation of MAP kinases. *Proc Natl Acad Sci USA*. 1997;94:9705–9710. doi: 10.1073/pnas.94.18.9705
29. Gan Z, Audi SH, Bongard RD, Gauthier KM, Merker MP. Quantifying mitochondrial and plasma membrane potentials in intact pulmonary arterial endothelial cells based on extracellular disposition of rhodamine dyes. *Am J Physiol Lung Cell Mol Physiol*. 2011;300:L762–L772. doi: 10.1152/ajplung.00334.2010
30. Michelakis ED, McMurtry MS, Wu X-C, Dyck JRB, Moudgil R, Hopkins TA, Lopaschuk GD, Puttagunta L, Waite R, Archer SL. Dichloroacetate, a metabolic modulator, prevents and reverses chronic hypoxic pulmonary hypertension in rats: role of increased expression and activity of voltage-gated potassium channels. *Circulation*. 2002;105:244–250.
31. Sankhe S, Manousakidi S, Antigny F, Arthur Ataam J, Bentebbal S, Ruchon Y, Lecerf F, Sabourin J, Price L, Fadel E, et al. T-type Ca2+ channels elicit pro-proliferative and anti-apoptotic responses through impaired PP2A/Akt1 signaling in PASMCs from patients with pulmonary arterial

hypertension. *Biochim Biophys Acta Mol Cell Res*. 2017;1864:1631–1641. doi: 10.1016/j.bbamcr.2017.06.018
32. Kawut SM, Horn EM, Berekashvili KK, Widlitz AC, Rosenzweig EB, Barst RJ. von Willebrand factor independently predicts long-term survival in patients with pulmonary arterial hypertension. *Chest*. 2005;128:2355–2362. doi: 10.1378/chest.128.4.2355
33. Mojiri A, Nakhaii-Nejad M, Phan WL, Kulak S, Radziwon-Balicka A, Jurasz P, Michelakis E, Jahroudi N. Hypoxia results in upregulation and de novo activation of von Willebrand factor expression in lung endothelial cells. *Arterioscler Thromb Vasc Biol*. 2013;33:1329–1338. doi: 10.1161/ATVBAHA.113.301359
34. Lertkiatmongkol P, Liao D, Mei H, Hu Y, Newman PJ. Endothelial functions of platelet/endothelial cell adhesion molecule-1 (CD31). *Curr Opin Hematol*. 2016;23:253–259. doi: 10.1097/MOH.0000000000000239
35. Frid MG, Kale VA, Stenmark KR. Mature vascular endothelium can give rise to smooth muscle cells via endothelial-mesenchymal transdifferentiation: in vitro analysis. *Circ Res*. 2002;90:1189–1196. doi: 10.1161/01.res.0000021432.70309.28
36. Hopper RK, Moonen JR, Diebold I, Cao A, Rhodes CJ, Tojais NF, Hennigs JK, Gu M, Wang L, Rabinovitch M. In pulmonary arterial hypertension, reduced BMPR2 promotes endothelial-to-mesenchymal transition via HMGA1 and its target slug. *Circulation*. 2016;133:1783–1794. doi: 10.1161/CIRCULATIONAHA.115.020617
37. Chanthick C, Kanlaya R, Kiatbumrung R, Pattanakitsakul SN, Thongboonkerd V. Caveolae-mediated albumin transcytosis is enhanced in dengue-infected human endothelial cells: a model of vascular leakage in dengue hemorrhagic fever. *Sci Rep*. 2016;6:31855. doi: 10.1038/srep31855
38. Dabral S, Pullamsetti SS. Vascular stiffness and mechanotransduction: back in the limelight. *Am J Respir Crit Care Med*. 2017;196:527–530. doi: 10.1164/rccm.201611-2254LE
39. Bertero T, Handen AL, Chan SY. Factors associated with heritable pulmonary arterial hypertension exert convergent actions on the miR-130/301-vascular matrix feedback loop. *Int J Mol Sci*. 2018;19:E2289.
40. Michelakis ED, McMurtry MS, Sonnenberg B, Archer SL. The NO - K+ channel axis in pulmonary arterial hypertension. Activation by experimental oral therapies. *Adv Exp Med Biol*. 2003;543:293–322.
41. Siddiqui MR, Komarova YA, Vogel SM, Gao X, Bonini MG, Rajasingh J, Zhao YY, Brovkovych V, Malik AB. Caveolin-1-eNOS signaling promotes p190RhoGAP-A nitration and endothelial permeability. *J Cell Biol*. 2011;193:841–850. doi: 10.1083/jcb.201012129
42. Ozkor MA, Quyyumi AA. Endothelium-derived hyperpolarizing factor and vascular function. *Cardiol Res Pract*. 2011;2011:156146. doi: 10.4061/2011/156146
43. Ouyang JS, Li YP, Li CY, Cai C, Chen CS, Chen SX, Chen YF, Yang L, Xie YP. Mitochondrial ROS-K+ channel signaling pathway regulated secretion of human pulmonary artery endothelial cells. *Free Radic Res*. 2012;46:1437–1445. doi: 10.3109/10715762.2012.724532
44. Rybalkin SD, Yan C, Bornfeldt KE, Beavo JA. Cyclic GMP phosphodiesterases and regulation of smooth muscle function. *Circ Res*. 2003;93:280–291. doi: 10.1161/01.RES.0000087541.15600.2B
45. Toyoda H, Saito M, Okazawa M, Hirao K, Sato H, Abe H, Takada K, Funabiki K, Takada M, Kaneko T, et al. Protein kinase G dynamically modulates TASK1-mediated leak K+ currents in cholinergic neurons of the basal forebrain. *J Neurosci*. 2010;30:5677–5689. doi: 10.1523/JNEUROSCI.5407-09.2010
46. Decher N, Wemhöner K, Rinné S, Netter MF, Zuzarte M, Aller MI, Kaufmann SG, Li XT, Meuth SG, Daut J, et al. Knock-out of the potassium channel TASK-1 leads to a prolonged QT interval and a disturbed QRS complex. *Cell Physiol Biochem*. 2011;28:77–86. doi: 10.1159/000331715
47. Chai S, Wan X, Nassal DM, Liu H, Moravec CS, Ramirez-Navarro A, Deschênes I. Contribution of two-pore K+ channels to cardiac ventricular action potential revealed using human iPSC-derived cardiomyocytes. *Am J Physiol Heart Circ Physiol*. 2017;312:H1144–H1153. doi: 10.1152/ajpheart.00107.2017